New age constraints on the break-up of Rodinia and amalgamation of southwestern Gondwana from the Choquequirao Formation in southwestern Peru

Eben Blake Hodgin[1]*, Victor Carlotto[2], Francis A. Macdonald[3], Mark D. Schmitz[4] and James L. Crowley[4]

[1]Department of Earth and Planetary Science, University of California, 307 McCone Hall, Berkeley, CA 94720, USA

[2]Universidad Nacional San Antonio Abad del Cusco UNSAAC, Avenida de la Cultura 733, Cusco, Peru

[3]Department of Earth Sciences, University of California, 2111 Webb Hall, Santa Barbara, CA 93106, USA

[4]Department of Geosciences, Boise State University, 1910 University Drive, MS 1535, Boise, ID 83725, USA

EBH, 0000-0002-6569-5232

*Correspondence: ebenblake@berkeley.edu

Abstract: The Choquequirao Formation is a >3 km-thick amphibolite-grade succession that outcrops in the Central Andes of southern Peru. To constrain its age and tectonostratigraphic setting, detrital zircon and metamorphic zircon, titanite, and rutile U–Pb isotopic analyses were conducted. Mantle-derived *c.* 640 Ma detrital zircons constrain the maximum age of the lower part of the succession and 550–490 Ma metamorphic zircon domains constrain its minimum age. The absence of early Paleozoic detrital zircons suggests that deposition predated early Paleozoic orogenesis in southwestern Gondwana. The close similarity of detrital zircon age spectra to those from sediments deposited on the Arequipa basement suggests that the Choquequirao Formation was deposited on the Arequipa Terrane. Metamorphic titanite dates are highly overdispersed, yet they overlap with *c.* 460 Ma peak metamorphism recorded by metamorphic zircon. Pb-loss pathways displayed by metamorphic titanite have a lower intercept that overlaps with *c.* 325 Ma metamorphic rutile, which corresponds to Hercynian orogenesis. A poorly constrained upper intercept of *c.* 510 Ma may correspond to Pampean and/or early Famatinian orogenesis. We interpret the Cryogenian–Ediacaran Choquequirao Formation as having been deposited during the opening of the Palaeo-Iapetus (Puncoviscana–Clymene) Ocean between eastern Arequipa and southern Kalahari prior to the subsequent collision with southwestern Amazonia during the Pampean Orogeny.

Supplementary material: Detailed U–Pb LA-ICP-MS and CA-ID-TIMS methods, and zircon, titanite and rutile LA-ICP-MS U–Pb, CA-ID-TIMS U–Pb, ID-TIMS U–Pb and trace element data are available at https://doi.org/10.6084/m9.figshare.c.6266972

Precambrian basement inliers from the Central Andes are scarce, limiting opportunities to gain insights into the tectonic history of the underlying terranes. With so few constraints, it is uncertain where the boundary is located between the Arequipa Terrane and the easternmost extent of the Amazon Craton (Cárdenas *et al.* 1997; Chew *et al.* 2008; Mišković *et al.* 2009; Reimann Zumsprekel *et al.* 2015; Hodgin *et al.* 2021*a*). The poorly studied Choquequirao Formation, which is an extensive amphibolite-grade igneous and metasedimentary succession exposed in the Eastern Cordillera of southern Peru (Fig. 1), can thus shed light on the boundary between the Arequipa Terrane and the Amazon Craton, as well as the timing of their amalgamation. In addition, the Choquequirao Formation can also provide an insight into earlier plate tectonic processes, such as rifting. The age, provenance and metamorphic history of the Choquequirao Formation can also provide insights into the tectonic history of supercontinent break-up and reassembly during the Neoproterozoic. Most palaeogeographical models suggest that the break-up of Rodinia (McMenamin and McMenamin 2001) occurred primarily during the Tonian–Ediacaran (Li *et al.* 2008; Merdith *et al.* 2017*a*, *b*; Zhao *et al.* 2018), whereas other models, suggest that break-up was not completed until the early–middle Cambrian (Karlstrom *et al.* 2018; Busch *et al.* 2021). Most palaeogeographical models invoke a multistage break-up of Rodinia (Merdith *et al.*

From: Hynes, A. J. and Murphy, J. B. (eds) 2023. *The Consummate Geoscientist: A Celebration of the Career of Maarten de Wit*. Geological Society, London, Special Publications, **531**, 301–321.
First published online February 10, 2023, https://doi.org/10.1144/SP531-2022-197

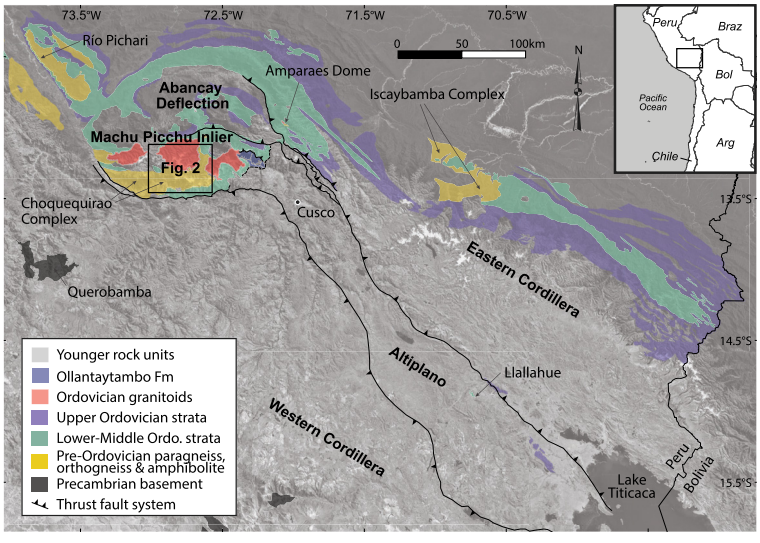

Fig. 1. Map of Ordovician and older geological units in southwestern Peru, modified after Chew *et al.* (2007*b*), Mišković *et al.* (2009), Reitsma (2012), Geological map quadrangles of Peru produced by INGEMMET at a scale of 1:100 000, and Hodgin *et al.* (2021*a*). Inset of western South America. Arg, Argentina; Bol, Bolivia; Braz, Brazil.

2017*a*; Robert *et al.* 2020; Evans 2021), yet geological evidence for multistage break-up from critical continental margins is challenging to identify (e.g. Thomas 1991; Eyster *et al.* 2018; Hodgin *et al.* 2022). In particular, ribbon terranes that formed by two rifting events (Lister *et al.* 1986; Péron-Pinvidic and Manatschal 2010) represent a unique opportunity to evaluate missing links within palaeogeographical models (e.g. Dalziel 1993, 1994; Li *et al.* 1995).

The Arequipa Terrane in southern Peru is commonly invoked as the conjugate rifted margin of eastern to southeastern Laurentia (e.g. Escayola *et al.* 2011; Casquet *et al.* 2012; van Staal *et al.* 2013; Ramacciotti *et al.* 2015; Rapela *et al.* 2016; Robert *et al.* 2020; Evans 2021); yet there is still a lack of clear geological evidence for rifting associated with a multistage break-up of Rodinia. Geological evidence related to a hypothesized accretion of the Arequipa Terrane to the Amazon Craton during the assembly of the supercontinent Gondwana is also sparse (Chew *et al.* 2008; Reimann Zumsprekel *et al.* 2015; Hodgin *et al.* 2021*a*). As a result, many tectonic models have suggested that the Arequipa Terrane was amalgamated to Amazonia in the Mesoproterozoic (Loewy *et al.* 2004; Chew *et al.* 2007*a*, *b*; Ramos 2008; Martin *et al.* 2020), implying that there may not be a Neoproterozoic Wilson Cycle preserved on the eastern margin of the Arequipa Terrane related to Rodinia dispersal and Gondwana amalgamation. Due to a lack of definitive geological evidence, a wide range of tectonic and palaeogeographical models have been put forward for the Arequipa Terrane that can be tested by investigating the age and provenance of the Choquequirao Formation.

Geological background

The Choquequirao Formation crops out in the Eastern Cordillera of the Central Andes in southern Peru (Fig. 1). It occurs within the Machu Picchu Inlier, which is itself part of the Abancay Deflection structural zone (Fig. 1) (Marocco 1978; Carlotto 2002; Carlotto *et al.* 2009). The name of the succession is derived from the important Inca archaeological site, Choquequirao, located centrally within the map area and whose metamorphic rocks were used to build the site (Carlotto *et al.* 2011). Only a handful of geological studies have been carried out within the remote, mountainous region containing the succession. The earliest studies by Heim (1948), Egeler and De Booy (1957, 1961) and Fricker and Weibel (1960) attributed the garnet-, sillimanite- and staurolite-bearing amphibolite-grade metamorphic rocks of the Choquequirao Formation to the Precambrian, whereas subsequent studies have generally assigned the succession to the early Paleozoic (Marocco 1978; Cárdenas *et al.* 1997; Carlotto *et al.* 1999, 2011).

The internal stratigraphy of the estimated 3.5 -km-thick Choquequirao Formation can be divided into five mappable stratigraphic units: (1) gneiss, amphibolite and diamictite; (2) massive quartzite and marble; (3) quartzo-feldspathic paragneiss; (4)

micaceous schist; and (5) quartzite and micaceous schist with marble (Cárdenas *et al.* 1997; Carlotto *et al.* 1999). The lowermost stratigraphic unit consists of gneiss, amphibolite and diamictite occurring within the cores of east–west-orientated anticlines and in the hanging walls of major thrust faults (Figs 2 & 3) (Marocco 1978; Cárdenas *et al.* 1997; Carlotto *et al.* 1999, 2011). The gneiss within the basal unit has been divided into orthogneiss and paragneiss lithologies, and it is associated with up to *c.* 1000 m of amphibolite, which itself may be derived from a combination of sedimentary and igneous protoliths (Cárdenas *et al.* 1997). The age of the basal gneiss is unknown but basal orthogneiss has been tentatively correlated with dated inliers at Río Pichari, *c.* 200 km to the NW, and at Amparaes Dome, *c.* 100 km to the NE (Fig. 1). A crystalline basement sample of charnockite from the Río Pichari Inlier, similar to the orthogneiss lithologies in the basal Choquequirao Formation (Cárdenas *et al.* 1997), yielded an upper intercept age of 1140 ± 30 Ma (Dalmayrac *et al.* 1977, 1988). Hornblende-rich orthogneiss in the basal unit has also been lithologically correlated to hornblende granite at Amparaes Dome (Fig. 1) (Cárdenas *et al.* 1997), which has been dated subsequently at 479 ± 2.3 Ma (Reitsma 2012). However, the presence of contact metamorphism, as indicated by garbenschiefer in the

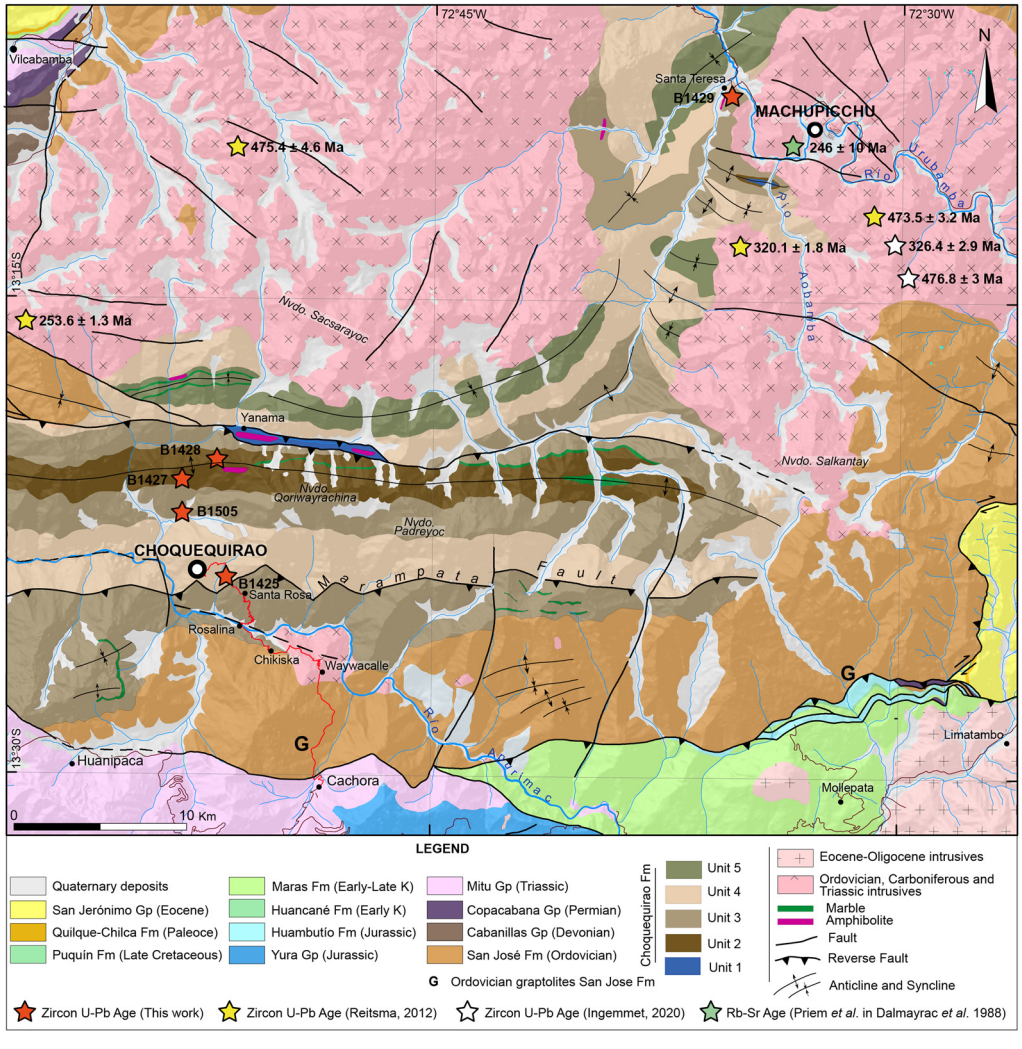

Fig. 2. Regional geological map between Choquequirao and Machu Picchu. Modified after Carlotto *et al.* (1999, 2011).

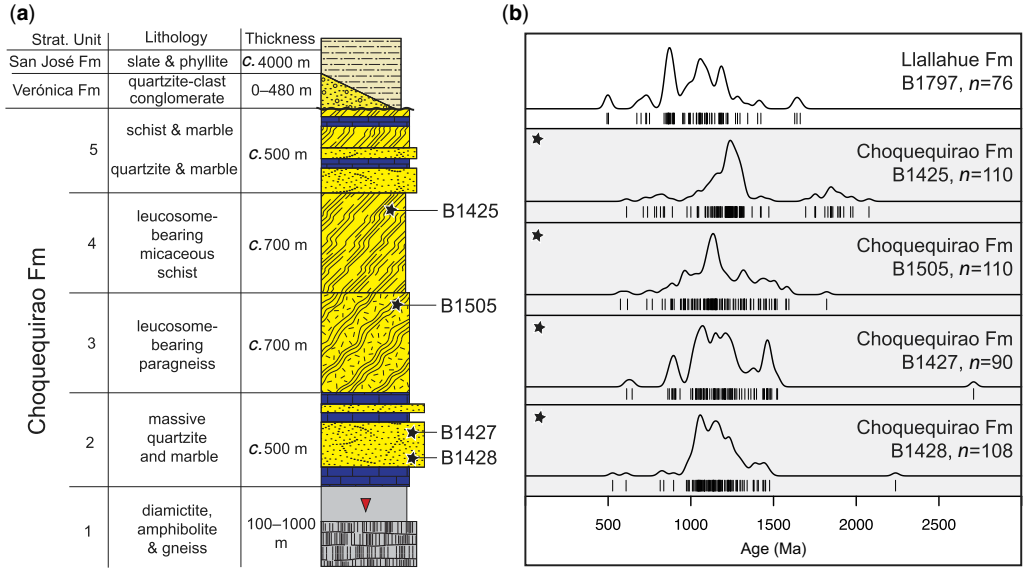

Fig. 3. (**a**) Schematic stratigraphy of the Choquequirao Formation. Unit thicknesses are modified after Carlotto *et al.* (1996), Cárdenas *et al.* (1997), Carlotto *et al.* (1999) and Martínez (1998). Detrital zircons samples indicated by black stars are located at their estimated stratigraphic position. (**b**) Kernel density and rug plots of four detrital zircon samples from the Choquequirao Formation and one detrital zircon sample from the Llallahue Formation (Hodgin *et al.* 2021*a*). Kernel density, 20 myr; *n* is the number of detrital zircon analyses in each sample. Fm, Formation.

metasedimentary rocks surrounding the granite at Amparaes Dome, suggests an intrusive relationship. Granites of similar age have now also been found to intrude metasedimentary rocks of the Choquequirao Formation (Reitsma 2012; INGEMMET 2020). As a result, the basal stratigraphic unit of the Choquequirao Formation is conservatively considered to consist primarily of amphibolite and associated paragneiss. Within the basal stratigraphic unit, we also report diamictite, which is particularly well exposed in the core of an anticline at Rio Aobamba (Figs 2 & 3). The diamictite, which consists primarily of granitoid clasts similar to the Cryogenian Chiquerío Formation in coastal southwestern Peru (Chew *et al.* 2007*b*), is likely to sit stratigraphically between the amphibolite of unit 1 and the overlying marble of unit 2.

The second lithostratigraphic map unit is estimated to be 500 m thick, and consists predominantly of massive quartzite and marble (Fig. 3) (Carlotto *et al.* 1999). The marble intervals generally occur near the base and top of the unit. The basal marble, which is best exposed in the core of an anticline between Nevado Padreyoc and Nevado Salkantay (Fig. 2), reveals that the estimated 100 m carbonate interval (Carlotto *et al.* 2009) should be considered a minimum thickness.

The overlying lithostratigraphic unit consists of an estimated 700 m of predominantly quartzo-feldspathic paragneiss. Upsection, the fourth stratigraphic unit consists of an estimated 700 m of micaceous schist. The fifth and uppermost lithostratigraphic unit consists of an estimated 500 m of quartzite and micaceous schist containing interbedded marble. There are no direct age constraints on any of the stratigraphic units.

Overlying the Choquequirao Formation in angular unconformity (Carlotto *et al.* 1999) is a generally less metamorphosed, fossil-bearing succession of slates, quartzites and conglomerate belonging to the lower Ordovician Verónica and San José formations (Egeler and De Booy 1961; Carlotto *et al.* 1999). There are substantial thickness and facies changes in the conglomeratic Verónica Formation (Egeler and De Booy 1961; Carlotto *et al.* 1996), which consists of quartzite clasts that are likely to have been derived from the underlying Choquequirao Formation, and which also implies an intervening metamorphic event. The Verónica Formation grades up into the overlying San José Formation (Egeler and De Booy 1961; Hodgin *et al.* 2021*a*), which consists predominantly of fossiliferous slate and phyllite (Fig. 3). The oldest biostratigraphic age constraints from strata overlying the Choquequirao Formation come from *c.* 479–478 Ma graptolites in the lower San José Formation (Gutiérrez-Marco *et al.* 2019). Deposition of the Choquequirao Formation is thus considered to

predate the *c.* 480–445 Ma Famatinian Orogeny (Pankhurst *et al.* 1998).

Given the age constraints, high metamorphic grade and lithology of the Choquequirao Formation, the succession has been tentatively correlated with other pre-Ordovician inliers in the Eastern Cordillera (Cárdenas *et al.* 1997; Carlotto *et al.* 1999, 2011; Hodgin *et al.* 2021*a*). In southern Peru, the Choquequirao Formation may be equivalent to the undated Iscaybamba Complex, which consists of orthogneiss, amphibolite, andesite, quartzite and schist (Fig. 1) (Laubacher 1978; Palacios *et al.* 1996; Chávez *et al.* 1997; Sánchez and Zapata 2003; Carlotto *et al.* 2009); to the Amparaes Dome, which consists of amphibolites, quartzites, sandstones, schists and marbles; to the upper Cambrian Llallahue Formation, which consists of quartzite and arkosic sandstone (Hodgin *et al.* 2021*a*); or to the Neoproterozoic Chiquerío and San Juan formations overlying the Arequipa basement in coastal southwestern Peru (Chew *et al.* 2007*b*). In central and northern Peru, the Choquequirao Formation could be equivalent to high-grade metasedimentary rocks of the Marañón and Huaytapallana complexes that were intruded and deformed at *c.* 480 Ma (Fig. 1) (Chew *et al.* 2007*a*, 2016; Cardona *et al.* 2009).

Methods

Zircon crystals were separated from geochronological samples using standard mineral separation procedures, then imaged with a cathodoluminescence (CL) detector and dated by laser ablation inductively coupled plasma mass spectrometry (LA-ICP-MS) at Boise State University (BSU) (see Supplementary Section S1 for details of the U–Pb zircon LA-ICP-MS geochronology methods). Metamorphic zircons were identified based on CL zonation, the Th/U ratio and Ti-in-Zr thermometry (Ferry and Watson 2007; Rubatto 2017). Zircon domains with Th/U values of less than 0.1 were generally identified as metamorphic (Rubatto 2017). Due to the prevalence of Pb loss in zircons from these high-grade and poly-deformed rocks, a younger cutoff of 900 Ma was used in reporting $^{206}Pb/^{238}U$ v. $^{207}Pb/^{206}Pb$ dates (e.g. Hodgin *et al.* 2022), and a concordance filter was set at −10 to +15%. The tectonomagmatic environment of the melt from which specific age populations of zircons crystallized was assessed using LA-ICP-MS zircon trace element indicators, such as U/Yb v. Nb/Yb (Grimes *et al.* 2015). The youngest detrital zircons in each sample identified by LA-ICP-MS were dated more precisely by chemical abrasion isotope dilution thermal ionization mass spectrometry (CA-ID-TIMS) at BSU (see Supplementary Section S1for details of the U–Pb zircon geochronology methods). Due to the prevalence of Pb loss in these high-grade poly-deformed rocks, most zircon crystals dated by CA-ID-TIMS were broken into multiple fragments in order to determine precisely the upper intercepts corresponding to the crystallization age and lower intercepts corresponding to the timing of Pb loss during peak metamorphism. Metamorphic rutile and titanite crystals were also analysed by LA-ICP-MS from sample B1425. A selection of titanite crystals were subsequently dated by ID-TIMS.

Comparative analysis of detrital zircon spectra was carried out using the IsoplotR software package (Vermeesch 2018). In addition to generating comparative kernel density (KDE) and cumulative age distribution (CAD) plots, datasets were quantitatively compared using the Kolmogorov–Smirnov (K–S) statistical difference. This method takes the maximum vertical distance between two CADs, and multiple values of which can then be plotted using multidimensional scaling (Vermeesch 2013). Age spectra from the Choquequirao Formation detrital zircon samples (this study) were first compared to compilations of detrital zircon data representative of the Arequipa Terrane in coastal southern Peru (Chew *et al.* 2007*b*), from the Altiplano of southern Peru (this study) and from the southwestern rifted margin of the Amazon Craton (Babinski *et al.* 2013; Harris 2020; Harris *et al.* 2023). Comparative analysis also included samples from high-grade metasedimentary rocks of the Huaytapallana and Marañón complexes in the Eastern Cordillera of central and northern Peru (Chew *et al.* 2007*a*, *b*, 2008, 2016; Cardona *et al.* 2009), which were divided into samples having either a pre-Pampean rift-related affinity or a post-Pampean orogenic affinity following the detrital zircon tectonostratigraphic methodology developed by Cawood *et al.* (2012). Samples from the Huaytapallana and Marañón complexes were included for comparative analysis if the youngest detrital zircon was within error of the Early Ordovician, the minimum age of the Choquequirao Formation. Samples were characterized as having an orogenic affinity if they were dominated by late Neoproterozoic–early Paleozoic age peaks and as having a rift-related affinity if the dominant age peaks instead consisted of older regional basement sources (e.g. >1 Ga). Southwestern Kalahari was included in our analysis as it has been identified as the most likely conjugate rifted margin to eastern Arequipa and related terranes (Rapela *et al.* 2016; Casquet *et al.* 2018). Specifically, we incorporated a compilation from Neoproterozoic rift-related detrital zircon of the Gariep Belt in southwestern Kalahari (Basei *et al.* 2005; Hofmann *et al.* 2015; Thomas *et al.* 2016) and from the Saldania Belt in southern Kalahari (Andersen *et al.* 2018). The same $^{206}Pb/^{238}U$ v. $^{207}Pb/^{206}Pb$ age cutoffs and concordance filtering described above were applied to all datasets.

Results

U–Pb zircon geochronology

One U–Pb igneous sample (B1429) and four U–Pb detrital zircon samples were analysed from the Choquequirao Formation. The four detrital zircon samples are described in stratigraphic order, followed by a detrital zircon sample (B1797) from the Llallahue Formation in the Altiplano of southern Peru, which was included for comparative analysis (Fig. 3b).

B1429 is a fine-grained biotite-rich quartzo-feldspathic gneiss within an amphibolite map unit near Santa Teresa (Fig. 2: 13.1417° S, 72.5954° W). Millimetre-scale foliation is defined by biotite and the sample displays deformation-induced myrmekite structures, which are typically associated with amphibolite-grade metamorphism in K-feldspar-bearing granitoids (Simpson and Wintsch 1989; Menegon *et al.* 2006). Abundant angular oxides and interstitial grains of potassium feldspar and quartz further support our interpretation of an igneous protolith. The sample yielded four very small zircons, only two of which could be analysed by LA-ICP-MS. The $^{207}Pb/^{206}Pb$ dates were *c.* 1900 and *c.* 1100 Ma, which are consistent with Precambrian detrital zircon dates recovered from the other samples in this study, and may be explained as inherited or entrained grains within a zircon-poor protolith.

B1428 is a sample of coarse-grained quartzite that comes from the basal quartzite map unit collected near the core of an anticline near Abra San Juan on the hiking trail from Maizal to Yanama (Figs 2 & 3: 13.3329° S, 72.8658° W). One hundred and eight analyses yielded a broad dominant population ranging from 1500 to 950 Ma with a primary peak at *c.* 1200 Ma, and secondary peaks at *c.* 1450 and *c.* 1000 Ma (see Supplementary Table S1). Minor populations occur at *c.* 2250, *c.* 800 and *c.* 600 Ma. The youngest detrital zircon was split into two fragments, which were each dated by CA-ID-TIMS. The analyses overlap with concordia but they do not overlap with each other and are interpreted as slightly discordant. A weighted mean $^{207}Pb/^{206}Pb$ date is 635.1 ± 1.4 Ma. Assuming a lower intercept of 460 Ma yields an upper intercept date of 638.7 ± 4.2 Ma (Fig. 4; see Supplementary Table S2).

B1427 is a sample of coarse-grained leucosome-bearing quartzo-feldspathic schistose gneiss collected from the basal quartzite of unit 2 along the trail from Maizal to Abra San Juan at 13.3434° S, 72.8817° W (Figs 2 & 3). Ninety-two analyses yielded a broad, dominant population ranging from 1500 to 900 Ma with peaks at *c.* 1450, *c.* 1200, *c.* 1100 and *c.* 950 Ma (see Supplementary Table S1). Notable minor populations occur at *c.* 600 and *c.* 2700 Ma. The youngest detrital zircon was split into two fragments, which were each dated by CA-ID-TIMS. The analyses do not overlap and are each slightly discordant. A weighted mean $^{207}Pb/^{206}Pb$ date is 627.9 ± 1.8 Ma. Assuming a lower intercept of 460 Ma, an upper intercept date is 639.5 ± 5.6 Ma (Fig. 4; see Supplementary Table S2).

B1505 is a sample of micaceous quartzo-feldspathic gneiss collected from the paragneiss map unit that overlies the basal quartzite map unit (Figs 2 & 3) (Carlotto *et al.* 1999). It was collected at Quebrada Victoria, also referred to as Río Blanco, at 13.3636° S, 72.8840° W. One analysis on a metamorphic zircon yielded a Th/U ratio of 0.01 and a date of 458.1 ± 23.2 Ma. The remaining 110 detrital zircon analyses yielded a broad dominant population ranging from 1500 to 900 Ma with a primary age peak at *c.* 1100 Ma, and secondary age peaks at *c.* 1450, *c.* 1300 and *c.* 950 Ma (see Supplementary Table S1). Minor populations occur at *c.* 1800, *c.* 1550, *c.* 850, *c.* 700 and *c.* 600 Ma. The youngest detrital zircon was split into three fragments dated by CA-ID-TIMS, resulting in discordant analyses that did not agree with each other. A weighted mean $^{207}Pb/^{206}Pb$ date is 635.1 ± 1.4 Ma. The three analyses resulted in an unanchored lower intercept date of 458.7 ± 13.8 Ma and an upper intercept date of 636.1 ± 8.6 Ma (mean squared weighted deviation (MSWD) = 1.2; probability of fit (POF) = 0.27). Assuming a lower intercept of 460 Ma yielded a similar upper intercept date of 636.8 ± 4.2 Ma (Fig. 4; see Supplementary Table S2).

B1425 is a sample of thin-bedded semi-pelitic quartzo-feldspathic quartzite collected near the 29 km marker along the trail from Marampata to the Choquequirao archeological site (Figs 2 & 3: 13.4011° S, 72.8573° W). Zircons from this sample were predominantly small and complex. Two metamorphic zircon domains with Th/U ratios of 0.07 and 0.08 yielded dates of 542 ± 41 and 496 ± 45 Ma, respectively. The analysed detrital zircon yielded a broad, dominant age population ranging from *c.* 1350 to *c.* 1100 Ma with a peak at *c.* 1250 Ma (see Supplementary Table S1). Secondary age populations occur at 2050–1700 Ma, *c.* 1450, *c.* 1000 and 900–700 Ma. Three of the youngest detrital zircon grains were dated by CA-ID-TIMS. Two of the grains (z1 and z2) fall on a discordia line with a lower intercept of 467.9 ± 17.6 Ma that is consistent with the age of Pb loss resolved by CA-ID-TIMS analyses in other samples, lending confidence to these two grains potentially sharing a common crystallization age defined by an upper intercept of 791.0 ± 4.5 Ma (Fig. 4; Supplementary Table S2). The remaining grain (z3) is located farther from concordia, and is likely to fall on a discordia line between peak metamorphism at *c.* 460 Ma and an early Neoproterozoic upper intercept age.

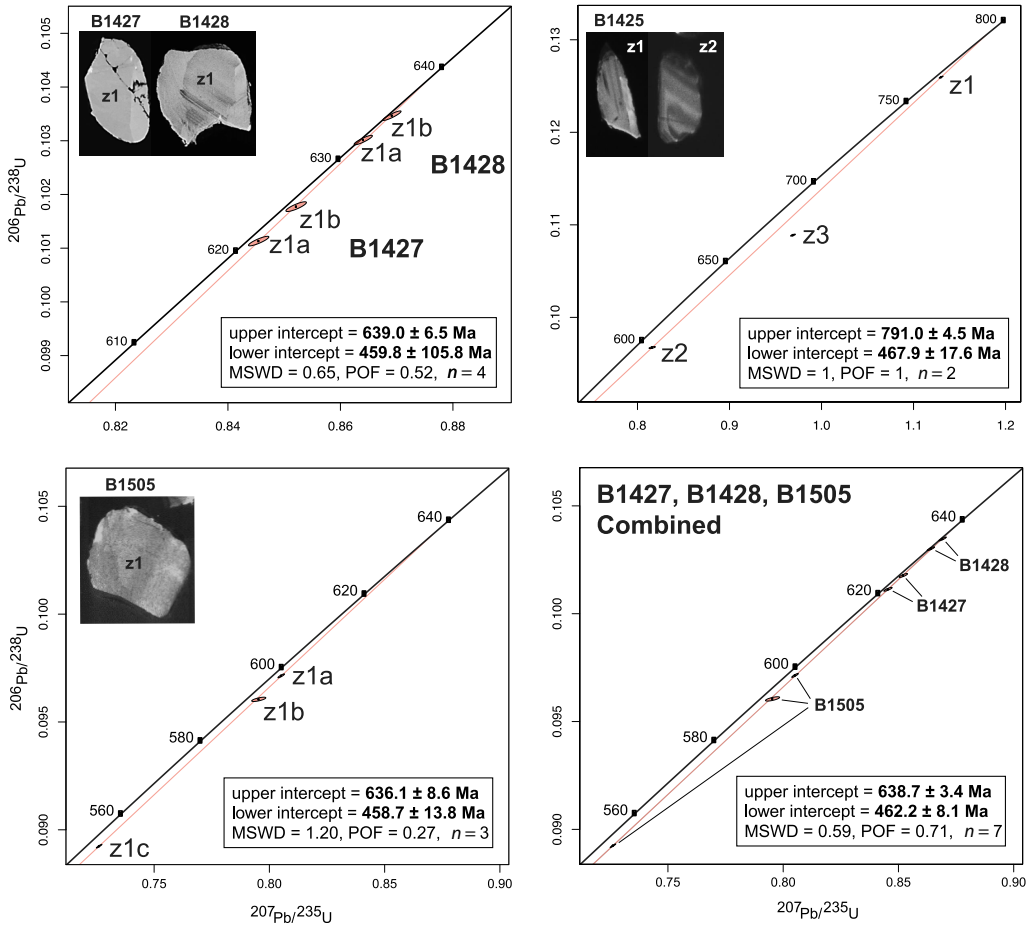

Fig. 4. Wetherill concordia plots of the youngest detrital zircons dated by CA-ID-TIMS from four Choquequirao Formation samples (B1425, B1427, B1428 and B1505). All upper and lower intercepts are unanchored. Insets show cathodoluminescence (CL) images of the dated zircons. MSWD, mean squared weighted deviation; POF, probability of fit; *n*, number of zircon fractions.

B1797 is a sample of arkosic sandstone from the upper Cambrian Llallahue Formation in the Altiplano of southern Peru (Figs 1–3) (Hodgin *et al.* 2021*a*). Due to its biostratigraphically well-constrained depositional age and its inferred tectonostratigraphic setting within an upper Cambrian back-arc basin (Hodgin *et al.* 2021*a*), this sample was included for comparison with detrital zircon samples from the Choquequirao Formation. LA-ICP-MS analyses resulted in 14 discordant dates and 76 concordant dates, of which the latter are included in our provenance analysis. The sample yielded a broad dominant population ranging from 1450 to 850 Ma with prominent age peaks at *c.* 1100 and *c.* 900 Ma (see Supplementary Table S1). Minor populations occur at *c.* 1650, 750–700 and *c.* 500 Ma. The three youngest detrital zircons from the *c.* 500 Ma population were dated by CA-ID-TIMS yielding $^{206}Pb/^{238}U$ dates of 496.75 ± 0.82, 500.11 ± 1.00 and 506.99 ± 3.01 Ma (see Supplementary Table S2). The youngest of these detrital zircon analyses from the Llallahue Formation (*c.* 497 Ma) constrains its maximum depositional age and is consistent with the trilobite fossils extracted from the same sample, which are early Furongian (Hodgin *et al.* 2021*a*), given that the base of the Furongian Epoch has a revised maximum depositional age of *c.* 494 Ma (Cothren e*t al.* 2022). These strata were thus deposited during approximately coeval magmatism.

U–Pb titanite geochronology

Sample B1425 (13.4011° S, 72.8573° W) contained lenticular-shaped titanite crystals characteristic of metamorphic titanite (Essex and Gromet 2000; Hodgin *et al.* 2021*b*). Twelve titanite crystals were

analysed by LA-ICP-MS (see Supplementary Table S3), and nine of these titanite crystals, which were split into 14 total titanite mineral fractions, were subsequently analysed by ID-TIMS (Fig. 5; Supplementary Table S4). A concordia-constrained 3D isochron using all analyses resulted in a well-resolved initial $^{207}Pb/^{206}Pb$ isotopic composition of 0.85219 and a lower-intercept age of 447.08 ± 0.32 Ma, approximately corresponding to the timing of peak metamorphism. We note that there is significant scatter in the ID-TIMS data, whose $^{206}Pb/^{238}U$ dates range from 465 to 430 Ma. The overdispersion and systematic discordance within the data suggest that the metamorphic titanite may record at least two Pb-loss pathways associated with earlier and later metamorphic events. Two apparent Pb-loss pathways displayed by the metamorphic titanite are both poorly constrained, yet the lower intercept overlaps with *c.* 325 Ma metamorphic rutile, which is likely to correspond to Hercynian orogenesis. A poorly constrained, upper intercept age of 508 ± 70 Ma overlaps with *c.* 540 and *c.* 490 Ma

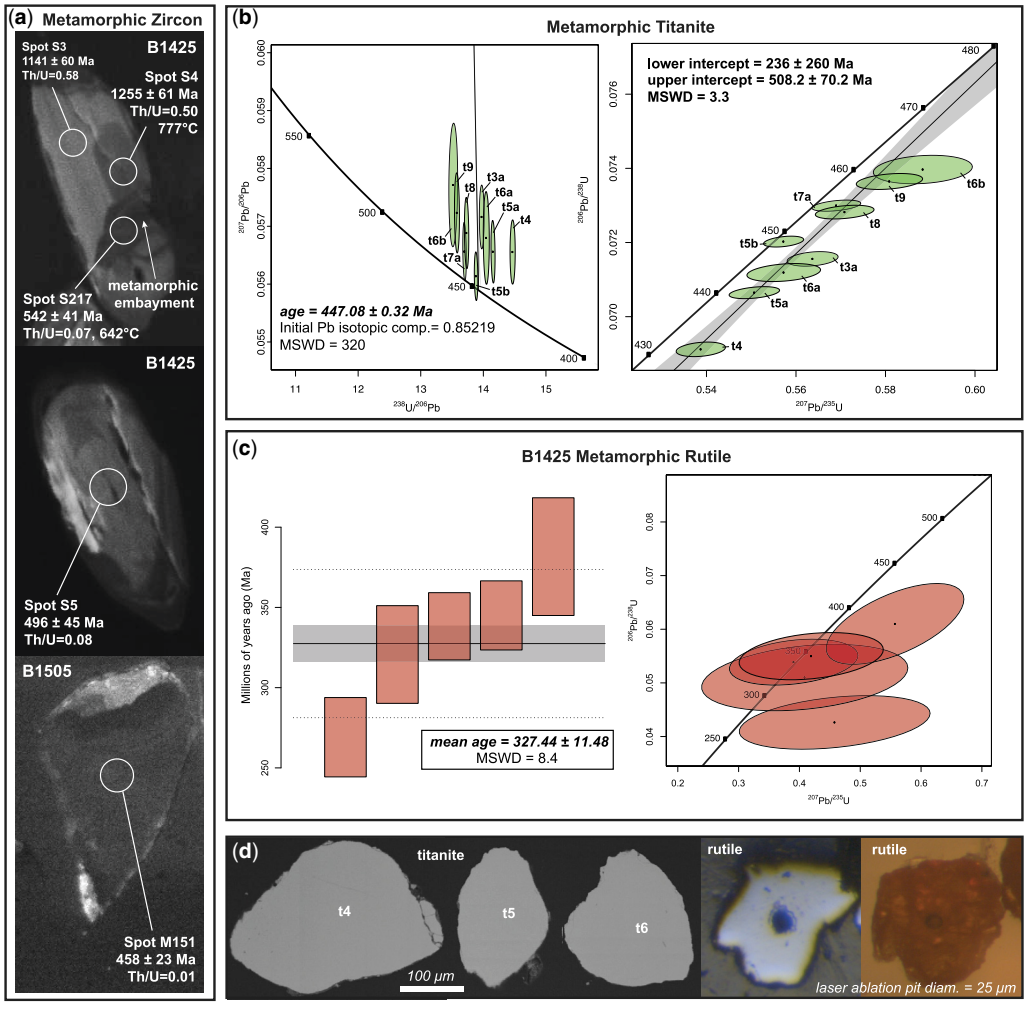

Fig. 5. Metamorphic petrochronology of the Choquequirao Formation. (**a**) Cathodoluminescence (CL) images of dated metamorphic zircon domains and entire grains. Laser ablation spot sizes are 25 µm. U–Pb dates, trace elements and Ti-in-Zr thermometry data can be found in Supplementary Table S1. (**b**) Tera Wasserburg (left) and Wetherill (right) concordia plots of metamorphic titanite ID-TIMS dates (see Supplementary Table S4). (**c**) Ranked age plot (left) and Wetherill concordia plot (right) of metamorphic rutile LA-ICP-MS dates (see Supplementary Table S5). (**d**) Backscattered electron images of metamorphic titanite crystals (left) and reflected and transmitted light images of a metamorphic rutile crystal (right).

metamorphic zircon (Fig. 5a), and may be related to Pampean and/or early Famatinian orogenesis.

Zr-in-titanite thermometry (Hayden *et al.* 2008; Kapp *et al.* 2009) on metamorphic titanite crystals resulted in temperatures of *c.* 700°C, which is consistent with amphibolite-grade peak metamorphism associated with leucosome generation and extensive migmatization in Choquequirao Formation metasedimentary rocks.

U–Pb rutile geochronology

Sample B1425 (13.4011° S, 72.8573° W) contained a population of rounded to prismatic rutile crystals ranging in diameter from 120 to 350 μm and hosting a variety of 10–20 μm-scale inclusions, with the most abundant identified optically and by CL as apatite, titanite and quartz. Five spot analyses were conducted from the centres of homogeneous and unfractured crystals (Fig. 5), yielding common Pb-corrected $^{206}Pb/^{238}U$ LA-ICP-MS dates with a weighted mean of 327.4 ± 11.5 Ma (Fig. 5; Supplementary Table S5), approximately corresponding to the age of high-grade 325–310 Ma metamorphism along the western Gondwana margin preserved at other localities in the Eastern Cordillera of central and northern Peru (Chew *et al.* 2007*a*, 2016; Cardona *et al.* 2009).

Discussion

Overview of the age and tectonic setting of the Choquequirao Formation

From previous studies it is known that the Choquequirao Formation predates cross-cutting Early Ordovician intrusions (Reitsma 2012; INGEMMET 2020) and also predates Early Ordovician deposition of the Verónica and San Jose formations, which unconformably overlie it (Egeler and De Booy 1961; Carlotto *et al.* 2011; Hodgin *et al.* 2021*a*). Previous mapping and reconnaissance of the Choquequirao Formation led to hypotheses that the depositional age of the succession may be Precambrian (Heim 1948; Fricker and Weibel 1960; Egeler and De Booy 1961) or early Paleozoic in age (Marocco 1978; Cárdenas *et al.* 1997; Carlotto *et al.* 1999, 2011; Hodgin *et al.* 2021*a*). Recent studies on potentially equivalent high-grade sedimentary complexes in central and northern Peru have revealed the presence of poorly differentiated Precambrian, early Paleozoic and late Paleozoic successions (Chew *et al.* 2007*a*, 2008, 2016; Cardona *et al.* 2009). To address uncertainty in the age of the Choquequirao Formation, we developed new ages from detrital zircon samples to constrain its maximum age, and new metamorphic ages to better constrain its minimum age and tectonic history. In addition, zircon trace element and provenance analyses were used to interpret the tectonostratigraphic setting of the Choquequirao Formation, and the identity of the underlying crust. Finally, these data were synthesized within a larger tectonic context to address the timing of the Rodinia supercontinent break-up and subsequent Gondwana supercontinent amalgamation.

Prior to putting forward our interpretations of these high-grade, poly-deformed rocks, we lay out five plausible tectonostratigraphic settings of the Choquequirao Formation: (1) a >800 Ma basin that predates the break-up of Rodinia; (2) a *c.* 800–550 Ma rift basin that formed on the margin of eastern Amazonia or western Arequipa during the break-up of Rodinia; (3) a collisional basin associated with the *c.* 550–525 Ma Pampean Orogeny postulated to extend into the Eastern Cordillera of Peru (Aceñolaza and Toselli 2009; Escayola *et al.* 2011); (4) a 510–490 Ma back-arc basin that formed during a magmatic lull between the Pampean and Famatinian orogenies (Hodgin *et al.* 2021*a*); and (5) a *c.* 492–480 Ma extensional basin that formed during an early pulse of the Famatinian Orogeny (e.g. Astini 2008; Weinberg *et al.* 2018). Finally, we acknowledge that other ages and basin types could be present and that more than one tectonostratigraphic interval may be captured within the thick and poorly defined Choquequirao Formation.

Maximum age constraints of the Choquequirao Formation

All four U–Pb detrital zircon samples in this study yielded minor populations of Neoproterozoic *in situ* ages ranging from 750 to 550 Ma, which were the youngest detrital zircon analyses in the samples. Due to analytical imprecision of the *in situ* analyses and a lack of control for Pb loss, the youngest detrital zircons were subsequently dated by CA-ID-TIMS to more precisely and accurately constrain the maximum age of the Choquequirao Formation. Three of the four samples each contained a single zircon that was split into multiple fragments, which resulted in non-overlapping dates that displayed Pb loss along a discordia line, and yielded upper intercept ages overlapping in uncertainty between 640 and 635 Ma. By assuming that these detrital zircon grains could represent a single age population, the CA-ID-TIMS analyses were combined to yield an upper intercept of 638.7 ± 3.4 Ma and a lower intercept of 462.2 ± 8.1 Ma (2σ, MSWD = 0.59, POF = 0.71). Combined, the statistical metrics (MSWD and POF) indicate an increased probability of derivation from a single age population. The zircons also displayed consistent crystal size, crystal morphology, CL response and zonation, and trace element profiles (Fig. 4; Supplementary Table S1). For

example, the U/Yb v. Nb/Yb tectonomagmatic fingerprinting proxy (Grimes *et al.* 2015) applied to all three zircons suggests a potentially common mantle-derived source (Fig. 6). On the basis of these factors, we interpret the upper intercept of 638.7 ± 3.4 Ma and the lower intercept of 462.2 ± 8.1 Ma as indicating that these grains from different samples may have shared a common igneous source and a common timing of peak metamorphism. The combined analyses and resulting intercept dates are thus interpreted as our most robust constraint on the maximum age of deposition and timing of peak metamorphism, respectively. The maximum age constraint of 638.7 ± 3.4 Ma pertaining to stratigraphic units 2 and 3 may be close to the age of deposition. This interpretation is supported by the presence of a glacial diamictite at Rio Aobamba in the basal stratigraphic unit that was likely to have been deposited during the *c.* 651–635 Ma Marinoan Snowball Earth glaciation (Hoffman *et al.* 1998; Nelson *et al.* 2020). An unconformity in the basal unit also means that the diamictite could have been deposited entirely or in part during the *c.* 717–660 Ma Sturtian Snowball Earth glaciation (Macdonald *et al.* 2010*a*; Rooney *et al.* 2015). From the combined geochronological and stratigraphic data, we infer that basal deposition of the Choquequirao Formation began during the 717–635 Ma Cryogenian Period. Based on the tectonomagmatic affinity of the *c.* 640 Ma detrital zircons, one potential source of mantle-derived detritus may be the basal amphibolite unit. However, geochemical characterization and direct dating of the amphibolites will be required to test this linkage and characterize the presence and timing of rift-related magmatism.

The provenance and tectonic setting of the Choquequirao Formation

In addition to information provided regarding the maximum age of deposition, the provenance of the four detrital zircon samples can be used to investigate the tectonic setting in which the succession was deposited (e.g. Cawood *et al.* 2012). To that end, observed trends within the four detrital zircon samples from the Choquequirao Formation are summarized and then compared to reference datasets from known tectonic setting.

Age spectra from all four samples are very similar, with the greatest similarity observed between the three basal samples (units 2 and 3 of the Choquequirao Formation). The three basal samples contained a broad, dominant age population ranging from 1500 to 900 Ma with peaks at *c.* 1450, *c.* 1200, *c.* 1100 and *c.* 950 Ma, and minor populations at *c.* 2700, *c.* 2250, *c.* 1800, *c.* 1550, *c.* 850, *c.* 700 and *c.* 600 Ma. The uppermost sample from unit 4 (B1425) had a somewhat more restricted dominant age population from *c.* 1350 to *c.* 1100 Ma with a well-defined peak at *c.* 1250 Ma, and secondary age populations at 2050–1700, *c.* 1450, *c.* 1000 and 900–700 Ma. The upper sample can be differentiated by having a more prominent 2050–1700 Ma age population, reduced abundance of *c.* 1100–950 Ma ages and an absence of the youngest *c.* 600 Ma population. We note that sample B1425

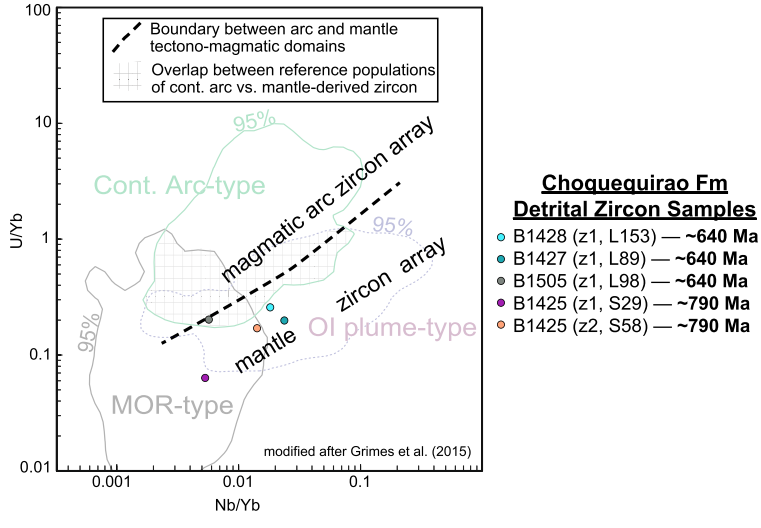

Fig. 6. Trace element fingerprinting of the youngest detrital zircons from the Choquequirao Formation. Tectonomagmatic fingerprinting using U/Yb v. Nb/Yb follows Grimes *et al.* (2015). LA-ICP-MS data can be found in Supplementary Table S1. Cont., Continental; MOR, mid-ocean ridge; OI, ocean island; Fm, Formation.

was finer grained than the three basal samples, which could have contributed to a minor redistribution of age population density according to grain size and transport distance within an overall common provenance (e.g. Leary *et al.* 2020). While there are minor differences, all four samples are interpreted as having a coherent provenance related to a strong likelihood of sharing a common crustal affinity and tectonic setting.

The age spectra of the four detrital zircon samples from the Choquequirao Formation were combined and compared with reference datasets of known tectonic setting (e.g. Cawood *et al.* 2012). Such a comparison indicates that the Choquequirao Formation follows detrital zircon age patterns associated with specific tectonic settings, and was thus likely to have been deposited in an extensional setting such as a rift basin or a passive margin, although an intraplate or back-arc setting cannot be ruled out. Due to the presence, but low percentage, of young detrital zircons in the three basal samples, a syndepositional magmatic source with low zircon fertility, as predicted in a rift setting, is most consistent with a rift basin (Cawood *et al.* 2012). Again, we note that this could also be consistent with a back-arc setting. In contrast, the uppermost sample, whose youngest detrital zircon is at least 150 myrs older than the time of deposition, may have more affinity with a passive margin setting or an intraplate setting. Due to the association of rift-related provenance signatures from the underlying strata, a passive margin setting is most probable, even though a back-arc setting is possible. The tectonic setting inferences are further supported by the lithostratigraphy of the Choquequirao Formation. The presence of basal amphibolites potentially related to rift-related volcanism and the apparent facies changes in the lowest stratigraphic units may be consistent with a rift–drift transition near the base of the Choquequirao Formation, possibly in unit 2. We also note that the age spectra of the Choquequirao Formation contrast with collisional to convergent basin settings, including back-arc settings, that are found regionally in slightly younger successions (Chew *et al.* 2007*a*, 2008, 2016; Cardona *et al.* 2009; Reimann Zumsprekel *et al.* 2015; Hodgin *et al.* 2021*a*). An enigmatic *c.* 640 Ma back-arc setting has been described by Escayola *et al.* (2007) in a potentially correlative tectonic position adjacent to the eastern margin of the Pampia Terrane in northwestern Argentina. We note the absence of late Neoproterozoic orogenic detritus in the Choquequirao Formation, which contrasts with abundant Neoproterozoic detritus in the succession described by Escayola *et al.* (2007). Thus, we interpret the provenance of the Choquequirao Formation as rift-related and predating latest Neoproterozoic–early Paleozoic orogenesis and associated basin development along the Gondwanan margin (Aceñolaza and Toselli 2009; Escayola *et al.* 2011). The uppermost unit of the Choquequirao Formation was not sampled, and it may represent a transition to another tectonostratigraphic setting that post-dates rift-related deposition.

Provenance analysis of the Choquequirao Formation to determine the identity of the underlying crust

The interpretation of the tectonic setting of the Choquequirao Formation as a rift to passive margin succession does not necessarily clarify the identity of the underlying crust. This is due to the uncertainty of the underlying crustal affinity in this region. The boundary between the easternmost extent of the Amazon Craton and the westernmost extent of the Arequipa Terrane in the Eastern Cordillera of Peru has been extensively debated (Cárdenas *et al.* 1997; Chew *et al.* 2007*a*, *b*, 2008; Mišković *et al.* 2009; Reimann *et al.* 2010; Reimann Zumsprekel *et al.* 2015; Hodgin *et al.* 2021*a*). By revealing age signatures that are potentially characteristic of basement sources from southeastern Amazonia or Arequipa, the provenance of the Choquequirao Formation can be used to determine the tectonic affinity of the underlying crust upon which the succession was deposited. One way to conduct such a test is to compare detrital zircon ages from the Choquequirao Formation to reference detrital zircon datasets derived from successions overlying basement of southwestern Amazonia and western Arequipa in coastal southern Peru. We also compare detrital zircon age spectra from the Choquequirao Formation to reference datasets from other successions in Peru.

As a result of our statistical analysis implementing the K–S distance between different detrital zircon datasets, the Choquequirao Formation is most similar to detrital zircon age spectra that are representative of the Arequipa Terrane in coastal southwestern Peru (Fig. 7) (Chew *et al.* 2007*b*). In particular, both detrital zircon compilations have a dominant population from 1300 to 950 Ma, minor 2000–1600 and 800–600 Ma populations, and a notable absence of detrital zircons from *c.* 1600 to 1450 Ma. In contrast, the Choquequirao Formation is least similar to age spectra from the compilations from southwestern Amazonia (Babinski *et al.* 2013; Harris 2020; Harris *et al.* 2023). The Amazonian compilations tend to have a greater abundance of >2000 Ma ages, a much more dominant 2000–1600 Ma population, significant 1600–1450 Ma populations that are absent from Arequipa, and subdued to minor Grenvillian age populations that tend to be the most dominant from Arequipa. The Choquequirao Formation also displays a high degree of

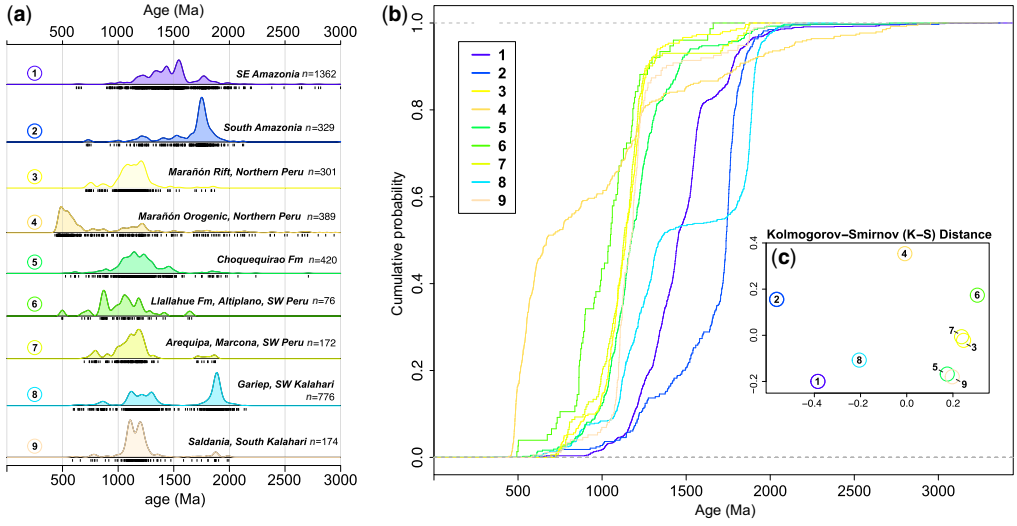

Fig. 7. Comparative analysis of Choquequirao Formation detrital zircon age spectra to detrital zircon age spectra from potentially correlative basins in Peru and potential conjugate rifted margins on the Amazon and Kalahari cratons. Plots were made using the IsoplotR software package (Vermeesch 2018). (**a**) Kernel density (KDE) plots from SW Amazonia (Harris 2020; Harris *et al.* 2023), South Amazonia (Babinski *et al.* 2013), Marañón rift affinity (Chew *et al.* 2007*a*, 2008, 2016; Cardona *et al.* 2009), Marañón orogenic affinity (Chew *et al.* 2007*a*, 2016; Cardona *et al.* 2009), Llallahue Formation, Altiplano SW Peru (this study), Arequipa, Marcona, SW Peru (Chew *et al.* 2007*b*), Gariep, SW Kalahari (Basei *et al.* 2005; Hofmann *et al.* 2015; Thomas *et al.* 2016) and Piketberg Formation, Saldania, South Kalahari (Andersen *et al.* 2018). We used a kernel bandwidth of 20 myr, a cutoff of 900 Ma to report $^{206}Pb/^{238}U$ v. $^{207}Pb/^{206}Pb$ dates and a $^{206}Pb/^{238}U$ v. $^{207}Pb/^{206}Pb$ concordance filter set at −10% to +15%. (**b**) Cumulative probability plot (CAD) of the age populations from each sample set plotted in (a). (**c**) Multidimensionally scaled plot of the Kolmogorov–Smirnov distances between the age populations from each sample set (Vermeesch 2013) in (a) and (b).

similarity with the upper Cambrian Llallahue Formation, which has been interpreted as having been deposited in a back-arc setting on Arequipa crust in the Altiplano of southern Peru (Hodgin *et al.* 2021*a*).

An additional linkage to an Arequipa provenance comes from the presence of 800–750 Ma mantle-derived zircons from the Choquequirao Formation (Fig. 6) and other early Paleozoic successions deposited on Arequipa (Reimann *et al.* 2010; Hodgin *et al.* 2021*a*). The common occurrence of mantle-derived 800–750 Ma detrital zircons on the Arequipa Terrane can be explained by their derivation from regional A-type Tonian–Cryogenian granitoid rocks in the Eastern and Western Cordillera of the Central Andes in Peru (Mišković *et al.* 2009) and on the southern continuation of the Arequipa Terrane (e.g. MARA Terrane) in northwestern Argentina (Colombo *et al.* 2009; Casquet *et al.* 2012). The most parsimonious interpretation of the detrital zircon comparative analysis is that the Choquequirao Formation, which is statistically similar to age spectra from the Arequipa Terrane, most probably had Arequipa basement as its primary source and was deposited on or near the eastern margin of the Arequipa Terrane.

Provenance analysis to determine the conjugate rifted margin to eastern Arequipa

Assuming that the Arequipa Terrane developed into a ribbon continent generated by two separate Neoproterozoic rifts during the break-up of Rodinia, it has generally been proposed that the eastern conjugate rifted margin is either southwestern Amazonia (Escayola *et al.* 2011; van Staal *et al.* 2013) or southwestern Kalahari (Rapela *et al.* 2016; Casquet *et al.* 2018). As discussed above, detrital zircon compilations from the rifted margin of southwestern Amazonia are dissimilar to detrital zircon compilations from the Choquequirao Formation, which does not support the model of southwestern Amazonia as a likely conjugate rifted margin of eastern Arequipa. Our analyses indicate a much greater statistical similarity between the Choquequirao Formation and the detrital zircon records from the rifted margins of southwestern Kalahari (Fig. 7). While there is a greater degree of statistical similarity between age spectra of the Choquequirao Formation and the Gariep Belt of southwestern Kalahari (Basei *et al.* 2005; Hofmann *et al.* 2015; Thomas *et al.* 2016), age spectra between the Saldania Belt (Andersen *et al.* 2018) and the Choquequirao Formation are so similar that

the two populations cannot be statistically differentiated (Fig. 7). This suggests that southwestern Kalahari, and in particular the Saldania Belt, could be the conjugate rifted margin of eastern Arequipa. This interpretation has been developed from other lines of geological evidence related to the Pampean Orogeny (Rapela *et al.* 2016; Casquet *et al.* 2018), including documentation of dextral shearing from *c.* 535 to 530 Ma (Iannizzotto *et al.* 2013; von Gosen *et al.* 2014) that could help to explain the dextral translation of Arequipa and related terranes. An earlier rift-related link is supported by additional geological evidence. Tonian–Cryogenian mantle-derived detrital zircons and regional occurrences of Tonian–Cryogenian intraplate magmatic sources on Arequipa and related terranes are similar to a large number of *c.* 880–750 Ma intraplate magmatic sources in southwestern Kalahari (Frimmel *et al.* 2001; Bartholomew 2008; Hanson *et al.* 2011; Will *et al.* 2020). These lines of evidence suggest a possible shared history of intraplate magmatism that may have developed earlier in southwestern Kalahari. We infer that protracted intraplate magmatism eventually led to successful Cryogenian–early Ediacaran rifting on the eastern margin of Arequipa, followed by successful late Ediacaran rifting on its western margin (Fig. 8) (Busch *et al.* 2022).

Possible continuation of the Arequipa Terrane into northern Peru

Detrital zircon samples from the high-grade metasedimentary rocks of the Huaytapallana and Marañón complexes in central and northern Peru contain contrasting age spectra (Chew *et al.* 2007*a*, 2008, 2016; Cardona *et al.* 2009) that are divided into samples having either a pre-Pampean rift-related affinity or a post-Pampean orogenic affinity (Chew *et al.* 2008; Cawood *et al.* 2012). The samples with an orogenic affinity contain prominent Paleozoic ages, tend to be dominated by latest Neoproterozoic–early Paleozoic age peaks, have comparatively reduced Mesoproterozoic age populations and contain a significant number of >2 Ga ages. In contrast, samples with a pre-orogenic or rift-related affinity from the Huaytapallana and Marañón complexes can be characterized as having pre-Pampean (e.g. >560 Ma) youngest detrital zircons, minor Neoproterozoic age peaks, a dominant late Mesoproterozoic age peak and rare occurrences of ages >2 Ga. Samples with an orogenic affinity incorporated into our comparative analysis include CM-228 and CM-112 (Cardona *et al.* 2009), AM076 (Chew *et al.* 2007*a*), and FW2-007 (Chew *et al.* 2016). Samples with a pre-orogenic rift-related affinity incorporated in our comparative analysis include CM-116 (Cardona *et al.* 2009), DC-05-5-4 (Chew *et al.* 2007*a*, 2008) and FW2-004 (Chew *et al.* 2016).

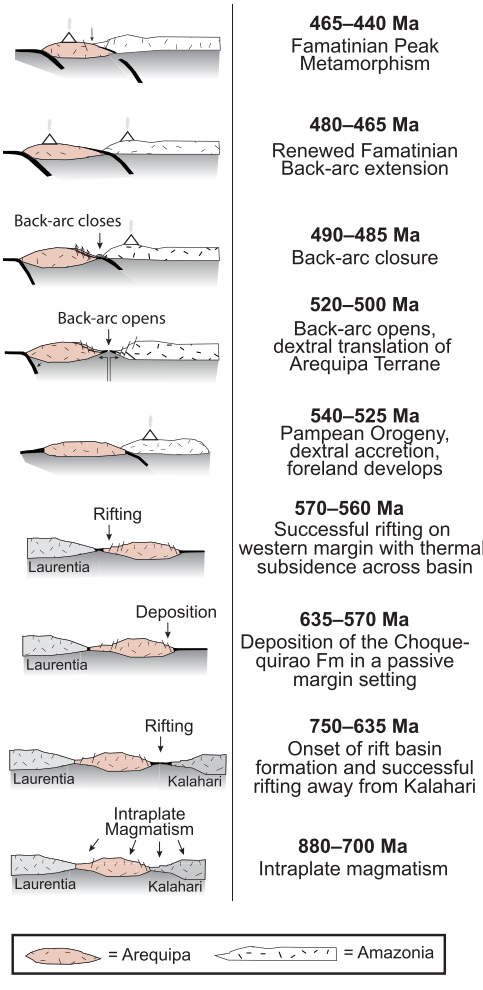

Fig. 8. Tectonic evolution block model of the Choquequirao Formation and the Arequipa Terrane in southwestern Peru.

The Huaytapallana and Marañón samples with a rift affinity agree very well statistically with samples from both the Arequipa Terrane (Marcona, Llallahue) and the Choquequirao Formation. In contrast, the age spectra of the rift-related samples are dissimilar to compilations of rift-related detrital zircon ages from southern and southwestern Amazonia (Fig. 7) (Babinski *et al.* 2013; Harris 2020; Harris *et al.* 2023). The simplest interpretation of the high-grade metasedimentary rock samples with a rift-related affinity in central and northern Peru is that they are most likely from rift-related strata deposited on the Arequipa Terrane. This suggests that the Arequipa Terrane may extend farther north into the Central Andes, even though the northern boundary of the Arequipa Terrane is generally

identified between southern and central Peru (e.g. Ramos 2008). We acknowledge that this suggestion is not consistent with mapped differences in whole-rock Pb isotopic signatures in Peru (Macfarlane *et al.* 1990), yet it is possible that Pb mobility in the mantle wedge associated with subduction throughout the Phanerozoic (Macfarlane *et al.* 1990 and references therein) may have played a larger role in resetting Pb crustal signatures in central and northern Peru. Further investigation from the Huaytapallana and Marañón complexes, and other Precambrian units, may help to better clarify the extent of the Arequipa Terrane, as well as the occurrence of early Paleozoic orogenic events.

Summary of the implications of the Choquequirao Formation on the break-up of Rodinia and the amalgamation of southwestern Gondwana

Rodinia break-up. The late Mesoproterozoic supercontinent of Rodinia was in the process of amalgamation and consolidation until *c.* 880 Ma and its break-up did not commence until *c.* 800 Ma (Li *et al.* 2008). The break-up of Rodinia was protracted and diachronous (Li *et al.* 2008) with the opening of interior oceans, such as the 650–550 Ma opening of the Iapetus Ocean (Robert *et al.* 2020) following earlier ocean-opening events from 800 to 650 Ma (Li *et al.* 2008). The diachronous fragmentation of Rodinia and delayed opening of the Iapetus Ocean are global developments in which the tectonic history of the Arequipa ribbon terrane can be situated. Increasingly, it has been put forward that the Iapetus Ocean opened in multiple events that may have generated rift-related ribbon continents such as the Arequipa Terrane (van Staal *et al.* 2013; Robert *et al.* 2020).

The timing of the initial opening of the Iapetus Ocean remains somewhat poorly constrained. It has been proposed that the eastern margin of Arequipa and related terranes underwent rifting as early as *c.* 925 Ma based on the youngest detrital zircon recovered from the Chilla Beds in Bolivia (Bahlburg *et al.* 2020) but this is inconsistent with the onset of Rodinia rifting at 800–750 Ma (Li *et al.* 2008; Merdith *et al.* 2017*a*), as well as the opening of the proposed conjugate rifted margin in southwestern Kalahari at 750–700 Ma (Macdonald *et al.* 2010*b*; Hofmann *et al.* 2014). The Chilla Beds may represent the eastern rifted margin of the Arequipa Terrane, except that the maximum depositional age is likely to be older than the true depositional age. As shown in detrital zircon studies of modern sediment, maximum depositional ages can be >100 myr older than the true depositional age, even in proximity to volcanic sources (Sharman and Malkowski 2020 and references therein).

Our detrital zircon analyses and revised lithostratigraphy from the Choquequirao Formation suggest that the succession represents rift-related deposits during the Cryogenian–Ediacaran. Affinity of the detrital zircon spectra with detrital zircon records from the Arequipa Terrane (see the previous subsection) support the interpretation that the Cryogenian–Ediacaran rift-related succession developed on the eastern margin of the Arequipa Terrane. Our comparative detrital zircon analysis further suggests that the Choquequirao Formation is most similar to rift-related detrital zircon records from the Gariep and Saldania belts of southwestern Kalahari, which may have been the conjugate rifted margin of eastern Arequipa. This reconstruction is supported by the presence of 850–750 Ma intraplate magmatism on Arequipa and its southern continuation (Colombo *et al.* 2009; Mišković *et al.* 2009; Casquet *et al.* 2012), and *c.* 800 Ma mantle-derived detrital zircons across the Arequipa Terrane (Hodgin *et al.* 2021*a*). Our precise maximum age constraints at *c.* 640 Ma represent significant new minimum age constraints on rift-related strata associated with the opening of an oceanic tract, which may be the northern extension of the Puncoviscana (Escayola *et al.* 2011) and Clymene oceans (Casquet *et al.* 2018). Our new age constraints overlap with other age constraints from the southern continuation of the Arequipa Terrane in northwestern Argentina, where early Ediacaran marbles dated at 635–620 Ma (Murra *et al.* 2016) and obducted oceanic crust dated at 647 ± 77 Ma (Escayola *et al.* 2007) constrain the opening of a Cryogenian–early Ediacaran oceanic tract.

Amalgamation of southwestern Gondwana. By dating metamorphic zircon, titanite and rutile, we identified multiple episodes of metamorphism within the poly-deformed, leucosome-bearing (formed by partial melting) Choquequirao Formation. Metamorphic zircon was dated by *in situ* spot analyses at *c.* 550, *c.* 490 and *c.* 460 Ma. Detrital zircons fragments dated by CA-ID-TIMS were used to precisely identify a primary Pb-loss event associated with peak metamorphism at *c.* 460 Ma. Owing, perhaps, to its lower closure temperature compared to zircon (Cherniak 1993), peak metamorphism in metamorphic titanite was identified by ID-TIMS at *c.* 445 Ma. The precise ID-TIMS titanite analyses exhibited significant overdispersion between 475 and 430 Ma, which could represent either a span of ages corresponding to distinct episodes of metamorphic crystallization during Famatinian orogenesis or Pb-loss pathways, which could be related to distinct metamorphic events prior to and following Famatinian metamorphism. Given that some titanite ID-TIMS

analyses that were generated from fragments of the same unzoned titanite crystals contributed to overdispersion, we favour the hypothesis that overdispersion is related primarily to Pb loss. This interpretation is supported by nearly all analyses being discordant and falling upon apparent Pb-loss pathways. Older dates on metamorphic zircon and younger dates on metamorphic rutile from the same sample (B1425) further suggest that overdispersion in our ID-TIMS titanite dataset is likely to be related to Pb loss.

First, we discuss the tectonic implications of well-resolved 460–440 Ma peak metamorphism in metamorphic zircon and titanite from the Choquequirao Formation. The timing of peak metamorphism recorded from *in situ* and isotope dilution zircon analyses is *c.* 460 Ma but peak metamorphic conditions arguably persisted for *c.* 20 myr, corresponding broadly to the final Oclóyic phase of Famatinian orogenesis (Pankhurst *et al.* 1998). We note that the initial timing of peak metamorphism may be associated with ophiolite emplacement in the central and northern Eastern Cordillera at 465 $\pm$ 24 Ma (Castroviejo *et al.* 2009, 2010; Rodrigues *et al.* 2010; Tassinari *et al.* 2011; Willner *et al.* 2014). The timing may correspond to the suturing of the Paracas Terrane (Ramos 2008). Alternatively, the ophiolitic crust in central and northern Peru could have originated in a back-arc basin that closed during the Famatinian Orogeny, which is the preferred tectonic model in the Eastern Cordillera of southern Peru (Bahlburg *et al.* 2006, 2011; Ramos 2008; Carlotto *et al.* 2009). The opening and closing of a back-arc basin is also consistent with our provenance results, which suggest the continuation of the Arequipa Terrane into central and northern Peru. Regardless, the highest temperature metamorphic conditions were likely to have been reached at the time of ophiolite emplacement at *c.* 465–460 Ma, followed by continued convergence associated with peak metamorphic conditions that persisted for *c.* 20 myr.

A separate upper Cambrian back-arc basin has recently been described in the Altiplano of southern Peru (Hodgin *et al.* 2021*a*). However, the upper Cambrian basin is capped by a significant Early Ordovician unconformity, and thus it appears to be unrelated to subsequent Middle–Late Ordovician back-arc formation and closure. Alternatively, in the better-studied type locality of the Famatinian Orogeny in northwestern Argentina, a separate pulse of intense back-arc extension has been documented (Wolfram *et al.* 2017) involving tholeiitic back-arc volcanism (Hauser *et al.* 2008; Coira *et al.* 2009; Bahlburg *et al.* 2016), leading to subsequent Middle–Late Ordovician back-arc closure and peak metamorphism during the Oclóyic phase of Famatinian orogenesis (Weinberg *et al.* 2018). Thus, we infer that protracted peak metamorphism at 460–440 Ma was probably caused by continued convergence associated with and following closure of a short-lived Famatinian back-arc basin.

Turning to pre-Famatinian metamorphism, we first discuss our results in the context of the limited geological evidence available for such metamorphic events. The deposition of quartzite clasts in the Lower Ordovician Verónica Formation (Hodgin *et al.* 2021*a*) implies that the underlying quartzites of the Choquequirao Formation, which are the most likely source of the clasts, had been metamorphosed prior to the Early Ordovician. The apparent Pb-loss discordia path in our metamorphic titanite dataset suggests that recrystallization and Pb loss followed an earlier metamorphic event. The poorly constrained upper intercept of *c.* 510 Ma overlaps with *c.* 550–490 Ma metamorphic zircon dates from the same sample (B1425). While we have some confidence in identifying at least one pre-Famatinian deformation event in the Choquequirao Formation rocks, we are unable at this time to disentangle the earlier metamorphic events with precision, which could be attributed to metamorphic overprinting, and in particular Famatinian peak metamorphism. As demonstrated from the Huaytapallana and Marañón complexes, the age of the metasedimentary rocks does not necessarily correlate with metamorphic grade, as amphibolite-grade metamorphic events associated with deposition of orogenic strata appear to have occurred during the Ordovician, Carboniferous and Permian (Chew *et al.* 2007*a*, 2016; Cardona *et al.* 2009). Further investigation will be required to tease apart evidence for pre-Famatinian tectonic events recorded within the poly-deformed rocks of the Choquequirao Formation.

The Choquequirao Formation also preserves a record of post-Famatinian deformation. Five U–Pb common Pb-corrected rutile *in situ* analyses yielded a weighted mean of 327.4 $\pm$ 11.5 Ma, which can be interpreted as recording a pulse of metamorphism during Hercynian metamorphism that is recorded elsewhere in the Eastern Cordillera at 325–310 Ma (Chew *et al.* 2007*a*, *b*, 2016; Cardona *et al.* 2009). Interestingly, this pulse of Carboniferous metamorphism is better expressed in the Marañón Complex of northern Peru than it is in the more proximal Huaytapallana Complex of central Peru, where Permian deformation is better preserved (Chew *et al.* 2007*a*, *b*, 2016). There is significant dispersion within our metamorphic rutile dataset, masked to a degree by relatively large analytical error. The oldest rutile crystal may thus record late-stage Famatinian metamorphism and the youngest rutile crystal may record Permian metamorphism (Fig. 5). These results highlight the preservation of multiple metamorphic events within poly-deformed rocks, and in individual samples and crystals, of the Choquequirao Formation.

Conclusions

The Choquequirao Formation (Formation) is a succession of amphibolite-grade igneous and metasedimentary rocks that crop out in a remote area of the Eastern Cordillera of the Central Andes in southern Peru. Three detrital zircon samples contain mantle-derived 640–635 Ma detrital zircons that constrain the maximum age of the lower part of the succession. The recognition of glacial diamictite in the basal strata of the Choquequirao Formation supports a Cryogenian basal age. The absence of early Paleozoic detrital zircons, which are by comparison common in the upper Cambrian–lower Ordovician Llallahue Formation and the Marañón and Huaytapallana complexes, suggests that deposition of the Choquequirao Formation predates the early Paleozoic orogenesis associated with the final amalgamation of Gondwana. The Choquequirao Formation is most likely to represent a Cryogenian–Ediacaran rift succession related to the break-up of Rodinia. The similarity of the Choquequirao Formation detrital zircon age spectra to the age of the Arequipa basement and to detrital zircons records from Neoproterozoic sedimentary rocks overlying the Arequipa Massif suggests that the Choquequirao Formation was deposited on the Arequipa Terrane, which we propose was its eastern rifted margin. Our detrital zircon compilation analysis indicates a high degree of similarity with pre-orogenic metasedimentary samples identified as rift-related from the Marañón and Huaytapallana complexes in central and northern Peru. This suggests that vestiges of the poorly exposed basement rock of the Arequipa Terrane may extend into northern Peru. Our analysis shows that southwestern Amazonia is an unlikely conjugate rifted margin to eastern Arequipa compared to southwestern Kalahari. The strong similarity between Choquequirao Formation age spectra and compiled data from the Saldania Belt in southern Kalahari supports a rift-related linkage within Rodinia reconstructions. Similar linkages between the Saldania Belt and the southern continuation of the Arequipa Terrane in NW Argentina (e.g. MARA Terrane) have been proposed previously (Rapela *et al.* 2016; Casquet *et al.* 2018).

Metamorphic titanite ID-TIMS dates display significant overdispersion along apparent Pb-loss pathways, yet a cluster of *c.* 470–430 Ma dates generally overlaps with *c.* 460 Ma peak metamorphism recorded by metamorphic zircon. The younger of two apparent Pb-loss pathways displayed by the metamorphic titanite has a lower intercept that overlaps with *c.* 325 Ma metamorphic rutile, probably corresponding to Hercynian orogenesis, which is recorded throughout the Eastern Cordillera (Chew *et al.* 2007*a*, 2016). The poorly constrained older upper intercept age of *c.* 510 Ma overlaps with 550–490 Ma metamorphic zircon and may be related to Pampean and/or early Famatinian orogenesis. An earlier phase of metamorphism is also indicated by a change in metamorphic grade across an angular unconformity between the quartzite-bearing Neoproterozoic Choquequirao Formation and the overlying quartzite-clast-bearing conglomerate of the lower Ordovician Verónica Formation (Hodgin *et al.* 2021*a*). These new data from the Choquequirao Formation may thus constrain the timing of the opening of the Palaeo-Iapetus (Puncoviscana–Clymene) Ocean in the Cryogenian–lower Ediacaran between the eastern margin of Arequipa and a conjugate rifted margin in southern Kalahari. Subsequently, Arequipa and related terranes collided with the Rio de la Plata and Amazon cratons during the Pampean Orogeny, which was followed by a series of Paleozoic orogenic events that are recorded in the polydeformed Choquequirao Formation.

Acknowledgments We are grateful to Tyler Barringer (SunPower Corporation) and Sam LoBianco (UC Santa Barbara) for field assistance; Janeth Cáceres for logistical support; Marion Lytle and Darin Schwartz (Boise State University) for analytical support; and Nicholas Swanson-Hysell for academic support to E.B. Hodgin. Constructive reviews from Victor Ramos and Cees van Staal helped to improve this paper.

Competing interests The authors declare that they have no known competing financial interests or personal relationships that could have appeared to influence the work reported in this paper.

Author contributions **EBH:** conceptualization (lead), investigation (lead), methodology (lead), formal analysis (lead), writing – original draft (lead), writing – review and editing (lead); **VC:** conceptualization (supporting), investigation (supporting), project administration (supporting), logistical support (lead), writing – original draft (supporting), writing – review and editing (supporting); **FAM:** funding acquisition (lead), resources (supporting), conceptualization (supporting), project administration (supporting), writing – review and editing (supporting); **MDS:** formal analysis (supporting), resources (lead), data curation (lead), methodology (supporting), software (supporting); **JLC:** formal analysis (supporting), methodology (supporting), data curation (supporting).

Funding This research received no specific grant from any funding agency in the public, commercial, or not-for-profit sectors.

Data availability All data generated or analysed during this study are included in the published article and in its supplementary information files.

Correction notice The publisher apologizes for including incorrect versions of Figures 2, 6 and 8. The correct figures have now been inserted.

References

Aceñolaza, F.G. and Toselli, A. 2009. The Pampean Orogen: Ediacaran–lower Cambrian evolutionary history of central and northwest region of Argentina. *In*: Gaucher, C., Sial, A.N., Halverson, G.P. and Frimmel, H.E. (eds) *Neoproterozoic–Cambrian Tectonics, Global Change and Evolution: A Focus on Southwestern Gondwana*. Developments in Precambrian Geology, **16**. Elsevier, Amsterdam, 239–254.

Andersen, T., Elburg, M.A., van Niekerk, H.S. and Ueckermann, H. 2018. Successive sedimentary recycling regimes in southwestern Gondwana: evidence from detrital zircons in Neoproterozoic to Cambrian sedimentary rocks in southern Africa. *Earth-Science Reviews*, **181**, 43–60, https://doi.org/10.1016/j.earscirev.2018.04.001

Astini, R.A. 2008. Sedimentación, facies, discordancias y evolución paleoambiental durante el Cambro-Ordovícico. *In*: Coira, B.L. and Zappettini, E.O. (eds) *Geología y recursos naturales de la provincia de Jujuy: relatorio: XVII Congreso Geológico Argentino: 7 al 10 de octubre de 2008, San Salvador de Jujuy*. Asociación Geológica Argentina, Buenos Aires, 50–73.

Babinski, M., Boggiani, P.C., Trindade, R.I.F.D. and Fanning, C.M. 2013. Detrital zircon ages and geochronological constraints on the Neoproterozoic Puga diamictites and associated BIFs in the southern Paraguay Belt, Brazil. *Gondwana Research*, **23**, 988–997, https://doi.org/10.1016/j.gr.2012.06.011

Bahlburg, H., Carlotto, V. and Cárdenas, J. 2006. Evidence of early to Middle Ordovician arc volcanism in the Cordillera oriental and Altiplano of southern Peru, Ollantaytambo Formation and Umachiri beds. *Journal of South American Earth Sciences*, **22**, 52–65, https://doi.org/10.1016/j.jsames.2006.09.001

Bahlburg, H., Vervoort, J.D., DuFrane, S.A., Carlotto, V., Reimann, C. and Cárdenas, J. 2011. The U–Pb and Hf isotope evidence of detrital zircons of the Ordovician Ollantaytambo Formation, southern Peru, and the Ordovician provenance and paleogeography of southern Peru and northern Bolivia. *Journal of South American Earth Sciences*, **32**, 196–209, https://doi.org/10.1016/j.jsames.2011.07.002

Bahlburg, H., Berndt, J. and Gerdes, A. 2016. The ages and tectonic setting of the Faja Eruptiva de la Puna Oriental, Ordovician, NW Argentina. *Lithos*, **256**, 41–54, https://doi.org/10.1016/j.lithos.2016.03.018

Bahlburg, H., Zimmermann, U., Matos, R., Berndt, J., Jimenez, N. and Gerdes, A. 2020. The missing link of Rodinia breakup in western South America: a petrographical, geochemical, and zircon Pb–Hf isotope study of the volcanosedimentary Chilla beds (Altiplano, Bolivia). *Geosphere*, **16**, 619–645, https://doi.org/10.1130/GES02151.1

Bartholomew, L.T. 2008. *Paleomagnetism of Neoproterozoic Intraplate Igneous Rocks in the Southwest Kalahari Craton, Namibia and South Africa*. Doctoral thesis, Texas Christian University, Fort Worth, Texas, USA.

Basei, M.A.S., Frimmel, H.E., Nutman, A.P., Preciozzi, F. and Jacob, J. 2005. A connection between the Neoproterozoic Dom Feliciano (Brazil/Uruguay) and Gariep (Namibia/South Africa) orogenic belts – evidence from a reconnaissance provenance study. *Precambrian Research*, **139**, 195–221, https://doi.org/10.1016/j.precamres.2005.06.005

Busch, J.F., Rooney, A.D., Meyer, E.E., Town, C.F., Moynihan, D.P. and Strauss, J.V. 2021. Late Neoproterozoic–early Paleozoic basin evolution in the Coal Creek inlier of Yukon, Canada: implications for the tectonic evolution of northwestern Laurentia. *Canadian Journal of Earth Sciences*, **58**, 355–377, https://doi.org/10.1139/cjes-2020-0132

Busch, J.F., Hodgin, E.B. *et al*. 2022. Global and local drivers of the Ediacaran Shuram carbon isotope excursion. *Earth and Planetary Science Letters*, **579**, 117368, https://doi.org/10.1016/j.epsl.2022.117368

Cárdenas, J.D., Carlotto, V.S., Romero, D., Jaimes, F. and Valdivia, W. 1997. *Geología de los cuadrángulos de Chuanquiri y Pacaypata, hojas: 26-py 27-p*. Boletín del Instituto Geológico, Minero y Metalúrgico, Serie A (Carta Geológica Nacional), **89**.

Cardona, A., Cordani, U.G., Ruiz, J., Valencia, V.A., Armstrong, R., Chew, D. and Nutman Sánchez, A.W. 2009. U–Pb zircon geochronology and Nd isotopic signatures of the pre-Mesozoic metamorphic basement of the eastern Peruvian Andes: growth and provenance of a late Neoproterozoic to Carboniferous accretionary orogen on the northwest margin of Gondwana. *The Journal of Geology*, **117**, 285–305, https://doi.org/10.1086/597472

Carlotto, V. 2002. *Évolution Andine et Raccourcissement au Pérou*. Geologie Alpine, Memoire Hors Série, **39**.

Carlotto, V., Gil, W., Cárdenas, J. and Chávez, R. 1996. *Geología de los cuadrángulos de Urubamba y Calca. Hojas: 27–r y 27-s*. Boletín del Instituto Geológico, Minero y Metalúrgico, Serie A (Carta Geológica Nacional), **65**.

Carlotto, V., Cárdenas, J.D., Romero, D., Valdivia, W. and Tintaya, D.D. 1999. *Geología de los cuadrángulos de Quillabamba y Machu Picchu*. Boletín del Instituto Geológico, Minero y Metalúrgico, Serie A (Carta Geológica Nacional), **127**.

Carlotto, V., Quispe, J. *et al*. 2009. Dominios geotectónicos y metalogénesis del Perú. Boletín de la Sociedad Geológica del Perú, **103**, 1–89.

Carlotto, V., Cárdenas, J., Fídel, L., Oviedo, M. and Pari, W. 2011. *Geología de Choquequirao*. Boletín del Instituto Geológico, Minero y Metalúrgico, Serie I (Patrimonio y Geoturismo), **4**.

Casquet, C., Rapela, C.W. *et al*. 2012. A history of Proterozoic terranes in southern South America: from Rodinia to Gondwana. *Geoscience Frontiers*, **3**, 137–145, https://doi.org/10.1016/j.gsf.2011.11.004

Casquet, C., Dahlquist, J.A. *et al*. 2018. Review of the Cambrian Pampean orogeny of Argentina; a displaced orogen formerly attached to the Saldania Belt of South Africa? *Earth-Science Reviews*, **177**, 209–225, https://doi.org/10.1016/j.earscirev.2017.11.013

Castroviejo, R., Rodrigues, J.F., Acosta, J., Pereira, E., Romero, D., Quispe, J. and Espí, J.A. 2009. Geología de las ultramafitas pre-andinas de Tapo y Acobamba, Tarma, Cordillera Oriental del Perú. *Geogaceta*, **46**, 7–10, https://oa.upm.es/11289/1/geogaceta_46.pdf

Castroviejo, R., Macharé, J. *et al*. 2010. *Significado de las ofiolitas Neoproterozoicas de la Cordillera Oriental del Perú (9°30′–11°30′). Resúmenes Extendidos XV*

Congreso Peruano de Geología, Cusco. Sociedad Geológica del Perú, Lima, 51–53.

Cawood, P.A., Hawkesworth, C.J. and Dhuime, B. 2012. Detrital zircon record and tectonic setting. *Geology*, **40**, 875–878, https://doi.org/10.1130/G32945.1

Chávez, A., Salas, G., Gutiérrez, E. and Cuadros, J. 1997. *Geología de los cuadrángulos de Corani y Ayapata, Hojas: 28-u, y 28-v*. Boletín del Instituto Geológico, Minero y Metalúrgico, Serie A (Carta Geológica Nacional), **90**.

Cherniak, D.J. 1993. Lead diffusion in titanite and preliminary results on the effects of radiation damage on Pb transport. *Chemical Geology*, **110**, 177–194, https://doi.org/10.1016/0009-2541(93)90253-F

Chew, D., Kirkland, C., Schaltegger, U. and Goodhue, R. 2007*a*. Neoproterozoic glaciation in the Proto-Andes: tectonic implications and global correlation. *Geology*, **35**, 1095–1098, https://doi.org/10.1130/G23768A.1

Chew, D.M., Schaltegger, U., Kosler, J., Whitehouse, M.J., Gutjahr, M., Spikings, R.A. and Mišković, A. 2007*b*. U–Pb geochronologic evidence for the evolution of the Gondwanan margin of the north-Central Andes. *Geological Society of America Bulletin*, **119**, 697–711, https://doi.org/10.1130/B26080.1

Chew, D.M., Magna, T., Kirkland, C.L., Mišković, A., Cardona, A., Spikings, R. and Schaltegger, U. 2008. Detrital zircon fingerprint of the Proto-Andes: evidence for a Neoproterozoic active margin? *Precambrian Research*, **167**, 186–200, https://doi.org/10.1016/j.precamres.2008.08.002

Chew, D.M., Pedemonte, G. and Corbett, E. 2016. Proto-Andean evolution of the Eastern Cordillera of Peru. *Gondwana Research*, **35**, 59–78, https://doi.org/10.1016/j.gr.2016.03.016

Coira, B., Kirschbaum, A., Hongn, F., Pérez, B. and Menegatti, N. 2009. Basic magmatism in northeastern Puna, Argentina: chemical composition and tectonic setting in the Ordovician back-arc. *Journal of South American Earth Sciences*, **28**, 374–382, https://doi.org/10.1016/j.jsames.2009.04.007

Colombo, F., Baldo, E.G. *et al*. 2009, A-type magmatism in the sierras of Maz and Espinal: a new record of Rodinia break-up in the Western Sierras Pampeanas of Argentina. *Precambrian Research*, **175**, 77–86, https://doi.org/10.1016/j.precamres.2009.08.006

Cothren, H.R., Farrell, T.P., Sundberg, F.A., Dehler, C.M. and Schmitz, M.D. 2022. Novel age constraints for the onset of the Steptoean Positive Isotopic Carbon Excursion (SPICE) and the late Cambrian time scale using high-precision U–Pb detrital zircon ages. *Geology*, **50**, 1415–1420, https://doi.org/10.1130/G50434.1

Dalmayrac, B., Lancelot, J.R. and Leyreloup, A. 1977. Two-billion-year granulites in the late Precambrian metamorphic basement along the southern Peruvian coast. *Science,* **198**, 49–51.

Dalmayrac, B., Laubacher, G. and Marocco, R. 1988. Caracteres generales de la evolución geológica de los Andes Peruanos. *Boletín del Instituto Geológico Minero y Metalúrgico, Serie D (Estudios especiales)*, **12**, 1–313.

Dalziel, I.W. 1993. Tectonic tracers and the origin of the proto-Andean margin. *In*: *XII Congreso Geológico Argentino y II Congreso de Exploración de Hidrocarburos, Volume 3*. Asociación Geológica Argentina, Buenos Aires, 367–374.

Dalziel, I.W. 1994. Precambrian Scotland as a Laurentia–Gondwana link: Origin and significance of cratonic promontories. *Geology*, **22**, 589–592, https://doi.org/10.1130/0091-7613(1994)022<0589:PSAALG>2.3.CO;2

Egeler, C.G. and De Booy, T. 1957. De geologisch-alpinistische exploratie in de Cordillera Vilcabamba en Cordillera Veronica, Zuidoost Peru. *Tijdschrift van het Aardrijkskundig Genootschap*, **74**, 120.

Egeler, C.G. and De Booy, T. 1961. Preliminary note on the geology of the Cordillera Vilcabamba (SE Peru), with emphasis on the essentially pre Andean origin of the structure. *Geologie en Mijnbouw*, **40**, 319–325.

Escayola, M.P., Pimentel, M.M. and Armstrong, R. 2007. Neoproterozoic backarc basin: Sensitive high-resolution ion microprobe U–Pb and Sm–Nd isotopic evidence from the Eastern Pampean Ranges, Argentina. *Geology*, **35**, 495–498, https://doi.org/10.1130/G23549A.1

Escayola, M.P., van Staal, C.R. and Davis, W.J. 2011. The age and tectonic setting of the Puncoviscana Formation in northwestern Argentina: an accretionary complex related to early Cambrian closure of the Puncoviscana Ocean and accretion of the Arequipa–Antofalla block. *Journal of South American Earth Sciences*, **32**, 438–459, https://doi.org/10.1016/j.jsames.2011.04.013

Essex, R.M. and Gromet, L.P. 2000. U–Pb dating of prograde and retrograde titanite growth during the Scandian orogeny. *Geology*, **28**, 419–422, https://doi.org/10.1130/0091-7613(2000)28<419:UDOPAR>2.0.CO;2

Evans, D.A. 2021. Pannotia under prosecution. *Geological Society, London, Special Publications*, **503**, 63–81, https://doi.org/10.1144/SP503-2020-182

Eyster, A., Ferri, F., Schmitz, M.D. and Macdonald, F.A. 2018. One diamictite and two rifts: Stratigraphy and geochronology of the Gataga Mountain of northern British Columbia. *American Journal of Science*, **318**, 167–207, https://doi.org/10.2475/02.2018.1

Ferry, J.M. and Watson, E.B. 2007. New thermodynamic models and revised calibrations for the Ti-in-zircon and Zr-in-rutile thermometers. *Contributions to Mineralogy and Petrology*, **154**, 429–437, https://doi.org/10.1007/s00410-007-0201-0

Fricker, P. and Weibel, M. 1960. Zur Kenntnis der Eruptive gesteine in der Cordillera Vilcabamba (Peru). *Schweizerrische Mineralogistche Petrologische Mitteilungen*, **40**, 359–382.

Frimmel, H.E., Zartman, R.E. and Späth, A. 2001. The Richtersveld Igneous Complex, South Africa: U–Pb zircon and geochemical evidence for the beginning of Neoproterozoic continental breakup. *The Journal of Geology*, **109**, 493–508, https://doi.org/10.1086/320795

Grimes, C.B., Wooden, J.L., Cheadle, M.J. and John, B.E. 2015. 'Fingerprinting' tectono-magmatic provenance using trace elements in igneous zircon. *Contributions to Mineralogy and Petrology*, **170**, 46, https://doi.org/10.1007/s00410-015-1199-3

Gutiérrez-Marco, J.C., Maletz, J. and Chacaltana, C.A. 2019. First record of lower Ordovician graptolites

from Peru. *In*: Obut, O.T., Sennikov, N.V. and Kipriyanova, T.P. (eds) *13th International Symposium on the Ordovician System: Contributions of International Symposium*. Publishing House of SB RAS, Novosibirsk, Russia, 59–62.

Hanson, R.E., Rioux, M. *et al*. 2011. Constraints on Neoproterozoic intraplate magmatism in the Kalahari Craton: Geochronology and paleomagnetism of c. 890–795 Ma extension-related igneous rocks in SW Namibia and adjacent parts of South Africa. *Geological Society of America Abstracts with Programs*, **43**(5), 371.

Harris, F.R. 2020. *'The Tale of 3000 zircons': An investigation of Grenville Sedimentiation in Amazonia using U/Pb Detrital Zircon Geochronology*. MSc dissertation, University of Kentucky, Lexington, Kentucky.

Harris, F.R., Moecher, D.P. and Tohver, E. 2023. Detrital zircon U–Pb provenance analysis of Precambrian and Paleozoic strata from southwestern Brazil: assessment of potential Grenvillian sediment input and Amazonian–Laurentian tectonic interaction. *Gondwana Research*, **113**, 14–30. https://doi.org/10.1016/j.gr.2022.09.017

Hauser, N., Matteini, M., Pimentel, M.M. and Omarini, R. 2008. Petrology and LA-ICPMS U–Pb geochronology of volcanic rocks of the Lower Paleozoic rock units of the Central Andes, NW Argentina: implications for the evolution of Western Gondwana. *In*: *Simposio; VI Simposio Sudamericano de Geología Isotópica; 2008, San Carlos de Bariloche, Argentina*. Instituto de Geocronología y Geología Isotópica, Buenos Aires (Proceedings CD-rom).

Hayden, L.A., Watson, E.B. and Wark, D.A. 2008. A thermobarometer for sphene (titanite). *Contributions to Mineralogy and Petrology*, **155**, 529–540, https://doi.org/10.1007/s00410-007-0256-y

Heim, A. 1948. *Geología de los ríos Apurímac y Urubamba*. Instituto Geologico del Peru, Lima.

Hodgin, E.B., Gutiérrez-Marco, J.C., Colmenar, J., Macdonald, F.A., Carlotto, V., Crowley, J.L. and Newmann, J.R. 2021*a*. Cannibalization of a late Cambrian backarc in southern Peru: new insights into the assembly of southwestern Gondwana. *Gondwana Research*, **92**, 202–227, https://doi.org/10.1016/j.gr.2021.01.004

Hodgin, E.B., Macdonald, F.A., Crowley, J.L. and Schmitz, M.D. 2021*b*. A Laurentian cratonic reference from the distal Proterozoic basement of Western Newfoundland using tandem in situ and isotope dilution U–Pb zircon and titanite geochronology. *American Journal of Science*, **321**, 1045–1079, https://doi.org/10.2475/07.2021.02

Hodgin, E.B., Macdonald, F.A., Karabinos, P., Crowley, J.L. and Reusch, D.N. 2022. A reevaluation of the tectonic history of the Dashwoods terrane using in situ and isotope-dilution U–Pb geochronology, western Newfoundland. Geological Society of America Special Papers, **554**, https://doi.org/10.1130/2021.2554(10)

Hoffman, P.F., Kaufman, A.J., Halverson, G.P. and Schrag, D.P. 1998. A Neoproterozoic snowball Earth. *Science*, **281**, 1342–1346, https://doi.org/10.1126/science.281.5381.1342

Hofmann, M., Linnemann, U., Hoffmann, K.H., Gerdes, A., Eckelmann, K. and Gärtner, A. 2014. The Namuskluft and Dreigratberg sections in southern Namibia (Kalahari Craton, Gariep Belt): a geological history of Neoproterozoic rifting and recycling of cratonic crust during the dispersal of Rodinia until the amalgamation of Gondwana. *International Journal of Earth Sciences*, **103**, 1187–1202, https://doi.org/10.1007/s00531-013-0949-6

Hofmann, M., Linnemann, U. *et al*. 2015. The four Neoproterozoic glaciations of southern Namibia and their detrital zircon record: the fingerprints of four crustal growth events during two supercontinent cycles. *Precambrian Research*, **259**, 176–188, https://doi.org/10.1016/j.precamres.2014.07.021

Iannizzotto, N.F., Rapela, C.W., Baldo, E.G., Galindo, C., Fanning, C.M. and Pankhurst, R.J. 2013. The Sierra Norte-Ambargasta batholith: Late Ediacaran–Early Cambrian magmatism associated with Pampean transpressional tectonics. *Journal of South American Earth Sciences*, **42**, 127–143, https://doi.org/10.1016/j.jsames.2012.07.009

INGEMMET 2020. *Geología del Batolito de la Cordillera Oriental entre 12°–15°S*. Datos Geocronológicos GR39B Geocatmin. Instituto Geológico, Minero y Metalúrgico (INGEMMET), Lima, http://metadatos.ingemmet.gob.pe:8080/geonetwork/srv/spa/resources.get?uuid=84fa3c20-3885-4c6c-8ba5-1473eff830dd&fname=Datos%20Geocronologia%20GR39B.zip&access=public

Kapp, P., Manning, C.E. and Tropper, P. 2009. Phase-equilibrium constraints on titanite and rutile activities in mafic epidote amphibolites and geobarometry using titanite–rutile equilibria. *Journal of Metamorphic Geology*, **27**, 509–521, https://doi.org/10.1111/j.1525-1314.2009.00836.x

Karlstrom, K., Hagadorn, J. *et al*. 2018. Cambrian Sauk transgression in the Grand Canyon region redefined by detrital zircons. *Nature Geoscience*, **11**, 438–443, https://doi.org/10.1038/s41561-018-0131-7

Laubacher, G. 1978. *Géologie de la Cordillère Orientale et de l'Altiplano au nord et nord-ouest du lac Titicaca (Pérou)*. Travaux et Documents de l'ORSTOM, **95**.

Leary, R.J., Smith, M.E. and Umhoefer, P. 2020. Grain-size control on detrital zircon cycloprovenance in the late Paleozoic Paradox and Eagle basins, USA. *Journal of Geophysical Research: Solid Earth*, **125**, e2019JB019226, https://doi.org/10.1029/2019JB019226

Li, Z.X., Zhang, L. and Powell, C.M. 1995. South China in Rodinia: part of the missing link between Australia–East Antarctica and Laurentia? *Geology*, **23**, 407–410.

Li, Z.X., Bogdanova, S. *et al*. 2008. Assembly, configuration, and break-up history of Rodinia: a synthesis. *Precambrian Research*, **160**, 179–210, https://doi.org/10.1016/j.precamres.2007.04.021

Lister, G.S., Etheridge, M.A. and Symonds, P.A. 1986. Detachment faulting and the evolution of passive continental margins. *Geology*, **14**, 246–250, https://doi.org/10.1130/0091-7613(1986)14<246:DFATEO>2.0.CO;2

Loewy, S.L., Connelly, J.N. and Dalziel, I.W. 2004. An orphaned basement block: the Arequipa–Antofalla Basement of the central Andean margin of South America. *Geological Society of America, Bulletins*, **116**, 171–187. https://doi.org/10.1130/B25226.1

Macdonald, F.A., Schmitz, M.D. *et al*. 2010*a*. Calibrating the cryogenian. *Science*, **327**, 1241–1243, https://doi.org/10.1126/science.1183325

Macdonald, F.A., Strauss, J.V., Rose, C.V., Dudás, F.Ő. and Schrag, D.P. 2010*b*. Stratigraphy of the Port Nolloth Group of Namibia and South Africa and implications for the age of Neoproterozoic iron formations. *American Journal of Science*, **310**, 862–888, https://doi.org/10.2475/09.2010.05

Macfarlane, A.W., Marcet, P., LeHuray, A.P. and Petersen, U. 1990. Lead isotope provinces of the Central Andes inferred from ores and crustal rocks. *Economic Geology*, **85**, 1857–1880, https://doi.org/10.2113/gsecongeo.85.8.1857

Marocco, R. 1978. *Un segment E–W de la Cordillera des Andes péruviaennes: La déflexion d'Abancay. Etude géologique de la Cordillère Orientale et des Hauts-plateaux entre Cuzco et San Miguel (Sud du Pérou)*. ORSTOM, Paris.

Martin, E.L., Spencer, C.J., Collins, W.J., Thomas, R.J., Macey, P.H. and Roberts, N.M.W. 2020. The core of Rodinia formed by the juxtaposition of opposed retreating and advancing accretionary orogens. *Earth-Science Reviews*, **211**, 103413, https://doi.org/10.1016/j.earscirev.2020.103413

Martínez, W. 1998. *El Paleozoico inferior en el Sur· del Perú: Estratigrafía cronostratigrafía, petrografía y aspectos sedimentológicos Región de Sandia*. Master's Thesis, Universidad Nacional Mayor de San Marcos, Lima, Peru.

McMenamin, M.A.S. and McMenamin, D.L.S. 2001. *The Emergence of Animals: The Cambrian Breakthrough*. Columbia University Press, New York.

Menegon, L., Pennacchioni, G. and Stünitz, H. 2006. Nucleation and growth of myrmekite during ductile shear deformation in metagranites. *Journal of Metamorphic Geology*, **24**, 553–568, https://doi.org/10.1111/j.1525-1314.2006.00654.x

Merdith, A.S., Collins, A.S. *et al*. 2017*a*. A full-plate global reconstruction of the Neoproterozoic. *Gondwana Research*, **50**, 84–134, https://doi.org/10.1016/j.gr.2017.04.001

Merdith, A.S., Williams, S.E., Müller, R.D. and Collins, A.S. 2017*b*. Kinematic constraints on the Rodinia to Gondwana transition. *Precambrian Research*, **299**, 132–150, https://doi.org/10.1016/j.precamres.2017.07.013

Mišković, A., Spikings, R.A., Chew, D.M., Košler, J., Ulianov, A. and Schaltegger, U. 2009. Tectonomagmatic evolution of Western Amazonia: geochemical characterization and zircon U–Pb geochronologic constraints from the Peruvian Eastern Cordilleran granitoids. *Geological Society of America Bulletin*, **121**, 1298–1324, https://doi.org/10.1130/B26488.1

Murra, J.A., Casquet, C., Locati, F., Galindo, C., Baldo, E.G., Pankhurst, R.J. and Rapela, C.W. 2016. Isotope (Sr, C) and U–Pb SHRIMP zircon geochronology of marble-bearing sedimentary series in the Eastern Sierras Pampeanas, Argentina. Constraining the SW Gondwana margin in Ediacaran to early Cambrian times. *Precambrian Research*, **281**, 602–617, https://doi.org/10.1016/j.precamres.2016.06.012

Nelson, L.L., Smith, E.F., Hodgin, E.B., Crowley, J.L., Schmitz, M.D. and Macdonald, F.A. 2020. Geochronological constraints on Neoproterozoic rifting and onset of the Marinoan glaciation from the Kingston Peak Formation in Death Valley, California (USA). *Geology*, **48**, 1083–1087, https://doi.org/10.1130/G47668.1

Palacios, O., Molina, O., Galloso, A. and Reyna, C. 1996. *Geología de los cuadrángulos de Puerto Luz, Colorado, Laberinto, Puerto Maldonado, Quincemil, Masuco, Astillero y Reserva Tambopata, Hojas: 26–u, 26-v, 26-x, 26-y, 27-u, 27-v, 27-x, 27-y*. Boletín del Instituto Geológico, Minero y Metalúrgico, Serie A (Carta Geológica Nacional), **81**.

Pankhurst, R.J., Rapela, C.W., Saavedra, J., Baldo, E., Dahlquist, J., Pascua, I. and Fanning, C.M. 1998. The Famatinian magmatic arc in the central Sierras Pampeanas: an Early to Mid-Ordovician continental arc on the Gondwana margin. *Geological Society, London, Special Publications*, **142**, 343–367, https://doi.org/10.1144/GSL.SP.1998.142.01.17

Péron-Pinvidic, G. and Manatschal, G. 2010. From microcontinents to extensional allochthons: witnesses of how continents rift and break apart? *Petroleum Geoscience*, **16**, 189–197, https://doi.org/10.1144/1354-079309-903

Ramacciotti, C.D., Baldo, E.G. and Casquet, C. 2015. U–Pb SHRIMP detrital zircon ages from the Neoproterozoic Difunta Correa Metasedimentary Sequence (Western Sierras Pampeanas, Argentina): Provenance and paleogeographic implications. *Precambrian Research*, **270**, 39–49, https://doi.org/10.1016/j.precamres.2015.09.008

Ramos, V.A. 2008. The basement of the Central Andes: the Arequipa and related terranes. *Annual Review of Earth and Planetary Sciences*, **36**, 289–324, https://doi.org/10.1146/annurev.earth.36.031207.124304

Rapela, C.W., Verdecchia, S.O. *et al*. 2016. Identifying Laurentian and SW Gondwana sources in the Neoproterozoic to Early Paleozoic metasedimentary rocks of the Sierras Pampeanas: Paleogeographic and tectonic implications. *Gondwana Research*, **32**, 193–212, https://doi.org/10.1016/j.gr.2015.02.010

Reimann, C.R., Bahlburg, H., Kooijman, E., Berndt, J., Gerdes, A., Carlotto, V. and López, S. 2010. Geodynamic evolution of the early Paleozoic Western Gondwana margin 14°–17°S reflected by the detritus of the Devonian and Ordovician basins of southern Peru and northern Bolivia. *Gondwana Research*, **18**, 370–384, https://doi.org/10.1016/j.gr.2010.02.002

Reimann Zumsprekel, C.R., Bahlburg, H., Carlotto, V., Boekhout, F., Berndt, J. and López, S. 2015. Multimethod provenance model for early Paleozoic sedimentary basins of southern Peru and northern Bolivia (13°–18° S). *Journal of South American Earth Sciences*, **64**, 94–115, https://doi.org/10.1016/j.jsames.2015.08.013

Reitsma, M.J. 2012. *Reconstructing the Late Paleozoic: Early Mesozoic Plutonic and Sedimentary Record of South-East Peru: Orphaned Back-Arcs along the Western Margin of Gondwana*. PhD thesis, University of Geneva, Geneva, Switzerland.

Robert, B., Domeier, M. and Jakob, J. 2020. Iapetan Oceans: an analog of Tethys? *Geology*, **48**, 929–933, https://doi.org/10.1130/G47513.1

Rodrigues, J., Acosta, J., Macharé, J., Pereira, E. and Castroviejo, R. 2010. *Evidencias estructurales de*

aloctonía de los cuerpos ultramáficos y máficos de la Cordillera Oriental del Perú en la región de Huánuco. Sociedad Geológica del Perú Publicación Especial, **9**, 75–78.

Rooney, A.D., Strauss, J.V., Brandon, A.D. and Macdonald, F.A. 2015. A Cryogenian chronology: two long-lasting synchronous Neoproterozoic glaciations. *Geology*, **43**, 459–462, https://doi.org/10.1130/G36511.1

Rubatto, D. 2017. Zircon: the metamorphic mineral. *Reviews in Mineralogy and Geochemistry*, **83**, 261–295, https://doi.org/10.2138/rmg.2017.83.9

Sánchez, A. and Zapata, A. 2003. *Memoria descriptiva de la revisión y actualización de los cuadrángulos de Sicuani (29-t), Nuñoa (29-u), Macusani (29-v), Limbani (29-x), Sandia (29-y), San Ignacio (29-z), Yahuri (30-t), Azángaro (30-v), Putina (30-x), La Rinconada (30-y), Condoroma (31-t), Ocuviri (31-u), Juliaca (31-v), Callalli (32-t) y Ácora (32-x), Escala 1:100.000*. Instituto Geológico, Minero y Metalúrgico, Lima.

Sharman, G.R. and Malkowski, M.A. 2020. Needles in a haystack: Detrital zircon U–Pb ages and the maximum depositional age of modern global sediment. *Earth-Science Reviews*, **203**, 103109, https://doi.org/10.1016/j.earscirev.2020.103109

Simpson, C. and Wintsch, R.P. 1989. Evidence for deformation-induced K-feldspar replacement by myrmekite. *Journal of Metamorphic Geology*, **7**, 261–275, https://doi.org/10.1111/j.1525-1314.1989.tb00588.x

Tassinari, C.C., Castroviejo, R., Rodrigues, J.F., Acosta, J. and Pereira, E. 2011. A Neoproterozoic age for the chromitite and gabbro of the Tapo ultramafic Massif, Eastern Cordillera, Central Peru and its tectonic implications. *Journal of South American Earth Sciences*, **32**, 429–437, https://doi.org/10.1016/j.jsames.2011.03.008

Thomas, R.J., Macey, P.H. *et al*. 2016. The Sperrgebiet Domain, Aurus Mountains, SW Namibia: a *c*. 2020–850 Ma window within the Pan-African Gariep Orogen. *Precambrian Research*, **286**, 35–58, https://doi.org/10.1016/j.precamres.2016.09.023

Thomas, W.A. 1991. The Appalachian–Ouachita rifted margin of southeastern North America. *Geological Society of America Bulletin*, **103**, 415–431, https://doi.org/10.1130/0016-7606(1991)103<0415:TAORMO>2.3.CO;2

van Staal, C., Chew, D. *et al*. 2013. Evidence of Late Ediacaran Hyperextension of the Laurentian Iapetan Margin in the Birchy Complex, Baie Verte Peninsula, Northwest Newfoundland: implications for the Opening of Iapetus, Formation of Peri-Laurentian Microcontinents and Taconic–Grampian Orogenesis. *Geoscience Canada*, **40**, 94–117, https://doi.org/10.12789/geocanj.2013.40.006

Vermeesch, P. 2013. Multi-sample comparison of detrital age distributions. *Chemical Geology*, **341**, 140–146, https://doi.org/10.1016/j.chemgeo.2013.01.010

Vermeesch, P. 2018. IsoplotR: a free and open toolbox for geochronology. *Geoscience Frontiers*, **9**, 1479–1493, https://doi.org/10.1016/j.gsf.2018.04.001

von Gosen, W., McClelland, W.C., Loske, W., Martinez, J.C. and Prozzi, C. 2014. Geochronology of igneous rocks in the Sierra Norte de Córdoba (Argentina): implications for the Pampean evolution at the western Gondwana margin. *Lithosphere*, **6**, 277–300, https://doi.org/10.1130/L344.1

Weinberg, R.F., Becchio, R., Farias, P., Suzaño, N. and Sola, A. 2018. Early Paleozoic accretionary orogenies in NW Argentina: growth of West Gondwana. *Earth-Science Reviews*, **187**, 219–247, https://doi.org/10.1016/j.earscirev.2018.10.001

Will, T.M., Höhn, S., Frimmel, H.E., Gaucher, C., Le Roux, P.J. and Macey, P.H. 2020. Petrological, geochemical and isotopic data of Neoproterozoic rock units from Uruguay and South Africa: correlation of basement terranes across the South Atlantic. *Gondwana Research*, **80**, 12–32, https://doi.org/10.1016/j.gr.2019.10.012

Willner, A.P., Tassinari, C.C., Rodrigues, J.F., Acosta, J., Castroviejo, R. and Rivera, M. 2014. Contrasting Ordovician high- and low-pressure metamorphism related to a microcontinent–arc collision in the Eastern Cordillera of Peru (Tarma province). *Journal of South American Earth Sciences*, **54**, 71–81, https://doi.org/10.1016/j.jsames.2014.05.001

Wolfram, L.C., Weinberg, R.F., Hasalová, P. and Becchio, R. 2017. How melt segregation affects granite chemistry: migmatites from the Sierra de Quilmes, NW Argentina. *Journal of Petrology*, **58**, 2339–2364, https://doi.org/10.1093/petrology/egy010

Zhao, G., Wang, Y., Huang, B., Dong, Y., Li, S., Zhang, G. and Yu, S. 2018. Geological reconstructions of the East Asian blocks: from the breakup of Rodinia to the assembly of Pangea. *Earth-Science Reviews*, **186**, 262–286, https://doi.org/10.1016/j.earscirev.2018.10.003